Geophys. J. R. astr. Soc. (1969) **17**, 121–149.

Non-Dipole Behaviour During an Upper Miocene Geomagnetic Polarity Transition in Oregon

N. D. Watkins

(Received 1968 November 27)*

Summary

The palaeomagnetism of a section of 71 successive lavas from south-eastern Oregon is presented. A geomagnetic polarity change from reversed to normal polarity which took place during the extrusion of the section 15 million years ago has allowed a palaeomagnetic examination of the non-dipole field during a period of diminished dipole intensity. During the polarity transition, there existed an apparent easterly-drifting non-dipole component. Together with an independent determination of the palaeo-intensity on one lava (Coe 1967) and other recently presented data (Goldstein *et al.* 1968) an application of Irving & Ward's (1964) geomagnetic field model to the data suggests a maximum dipole intensity as low as two per cent of the present value for a period of not less than 100 years during the transition, outside of which the data are consistent with some present-day ratios of non-dipole to dipole field intensity. A very short period of diminished relative dipole intensity occurred during the final stages of the polarity change, when the virtual geomagnetic pole returned to very low latitudes, without any polarity change actually occurring. Because of a great similarity with an independently presented result, it is suggested that this ' rebound effect ' may reflect a fundamental aspect of the mechanism of at least some polarity changes.

Comparison with estimates of the duration of some more recent geomagnetic polarity transitions suggests that the section may have accumulated in less than 50 000 years. The lavas of normal polarity, which comprise most of the section, do not show any preferred association with lower or higher oxidation states.

Introduction

The Earth's magnetic field is subject to fluctuations of several types, ranging from very short period variations of external origin, to changes with periods very much in excess of the duration of direct observations, the earliest of which probably began in China over one thousand years ago (Smith & Needham 1967).

Spherical harmonic analysis of the present geomagnetic field defines a major dipole component (*Fo*) which is quasi-permanent and at present inclined at 11° to the spin axis, and a more rapidly moving non-dipole component (*Fd*) which causes the secular variation, and which has been observed to move westward at about 0·2° of longitude per year (Bullard *et al.* 1950). This non-dipole component comprises

* Received in original form 1968 October 3.

from 0 to over 30 per cent of the present total field intensity. Kahle *et al.* (1967) have pointed out the complexity and variability of the present non-dipole drift. Cox (1962) earlier demonstrated the geographical variability of the non-dipole component by showing its virtually complete absence from most of the central Pacific region. McDonald & Gunst (1968) have recently emphasized the existence and changing nature of the geomagnetic field's hemispheric dissymetry.

Archaeomagnetic and palaeomagnetic methods have enabled indirect extension of observatory data. Aitken *et al.* (1964) have shown that the European secular variation is not regular in its movement over the past 2000 years. Doell & Cox (1965) have shown that the lack of secular variation in the central Pacific has persisted for as much as 100 000 years. They also suggest (Cox & Doell 1964) a periodicity of the geomagnetic field of about 100 000 years, which is termed random walk or dipole wobble. Dubois (1967) and Kawai *et al.* (1967), believe that the surface expression of the dipole wobble follows a clover-leaf pattern. Estimates of the time required to average this dipole wobble to the axial dipole field range from 10 000 years (Runcorn 1959) to one million years (Currie *et al.* 1963). The problem of averaging observations to the axial dipole is stressed by Grommé (1965) and Heinrichs (1967) who believe that there have existed periods characterized by large variations in direction of the geomagnetic field. Cox (1966) has shown that a large increase in the probable non-dipole to dipole field ratio in Alaska has produced geomagnetic field directions so divergent that an equatorial virtual geomagnetic pole exists locally in lavas less than 0·7 million years old, without the lavas being transitional between opposite polarities. Doell (1968) has recently presented evidence for similarly divergent geomagnetic directions without a polarity change, with the probable cause being a movement of the dipole field.

Palaeomagnetic methods have established beyond doubt that the geomagnetic field polarity has changed frequently, perhaps as many as 60 times during the past 13 million years (Dagley *et al.* 1967). McMahon & Strangway (1967) believe that the directions of constant polarity appear to last the order of 0·01, 0·10 and 50 million years, although shorter durations have been suspected by observation (Ninkovitch *et al.* 1966, Watkins 1968a), and by theoretical reasoning (Cox 1968).

Several lines of evidence relevant to the duration of the finite time of transition between opposite stable polarities are available, and these provide suggested limits of 2000 to 20 000 years for the transition (summary by Watkins 1965a). Cox & Dalrymple (1967) show by analysis of available K : Ar and polarity data for the period 0 to 4·0 m.y. that the best average time required for each of the nine known polarity transitions in that period is 4600 years, with 95 per cent confidence limits at 1000 and 21 000 years. Experimental determinations of the intensity of the geomagnetic field during a polarity transition are understandably rare. Intensities of the order of 10 to 30 per cent of the present values have been measured (Coe 1967) suggesting that perhaps at least the non-dipole field remains in existence during the transition process (Smith 1967). If this is so, then the non-dipole field behaviour would be isolated for examination during the period of polarity transition, and would ideally be reflected in directional departures from the palaeomeridians connecting the opposite stable pole positions, and relatively rapid movement.

All palaeomagnetic methods suffer from the fact that observations are only spot determinations in time. It follows therefore that the most suitable palaeomagnetic materials (basalts) can only be used to evaluate detailed behaviour if collected from sequences of lava flows (representing successive points in time) which have accumulated without major time breaks.

It is the purpose of this communication to present the palaeomagnetic results from a section of Upper Miocene lavas which were extruded in relatively rapid succession shortly before, during, and after a change of geomagnetic polarity from reversed to normal polarity.

The geology of Steens Mountain

Steens Mountain is the highest point and eastern edge of a great westerly dipping block in that part of the Basin and Range province which extends into southern Oregon. It is by far the largest topographic feature of the Great Basin, reaching over 3000 m above sea level, providing almost 2000 m of local relief in the form of a very steep fault scarp, above the Alvord Desert to the east.

Fuller (1931) has described the geology of Steens Mountain in detail. It consists of two greatly contrasting divisions. The oldest part of the lower division comprises a thick Middle Miocene (Fuller 1931, p. 43) tuffaceous series called the Alvord Creek Beds (which are in places diversified and locally deformed by a laccolith), a very thick sill, basic and salic andesites, and intermediate tuffs. Completing the lower half of the section are 150 m of rhyolitic flows and two locally thick dacitic flows interdigitated with tuffs, all of which are capped by a large series of thin aphanitic andesitic flows which vary greatly in thickness laterally.

In contrast, the upper division of the Steens Mountain section consists of a 1000 m thick monotonous series of regular lava flows lying unconformably over the irregular andesitic flows and cones. The lavas are thin, averaging only about 5 m in thickness. Interbasaltic sediments are absent, providing an impression of rapid accumulation. There exists no evidence to indicate that the lavas did not accumulate as the result of extrusions at regular short intervals. These are the type ' Steens Basalt ' lavas which are for the most part high alumina, coarsely porphyritic, diktytaxitic (microvesicular) basalts. The tectonic events which gave rise to the Steens scarp have also tilted the section up to 11° at N 286° E. This dip diminishes to zero about 500 m below the summit.

The entire mountain has been heavily glaciated, and small cirques exist at the head of several creeks which drain eastward down the fault scarp, the slope of which decreases drastically towards the base of the Steens Basalt where smaller cirques also occur. The glaciation has helped produce a series of excellent outcrops, in which large successions of lavas may be sampled. A particularly good example is found at the northern forks of the head of Alvord Creek, immediately below the summit of the mountain, as illustrated by Fuller (1931, p. 101, Fig. 60). Large slump blocks are found on the lower parts of the scarp, particularly where the incompetent tuffaceous beds exist, but such slumping has not presented any major difficulty in sampling, although accessibility was only accomplished by crossing from the northernmost fork of Alvord Creek southwards down the section.

Previous work

Evernden & James (1964) have placed lower limits on the age of the Steens Mountain section by obtaining K : Ar ages of 14·5 million years for a lava lapping onto the section, and 15·0 million years for a lava towards the top of the section. These data agree with the vertebrate palaeontological ages obtained from volcanically derived sediments southwest of Steens Mountain (Walker & Repenning 1965).

Watkins (1963, 1965b) included samples from the youngest 22 lavas at Steens summit in a regional survey of the Miocene lavas of the Columbia Plateaus. The data from southeastern Oregon (Watkins 1963) suggested that the thick sections of lava accumulated in a relatively short time. This indicates that the lavas are highly amenable to study of Miocene geomagnetic secular variation, if sufficient samples are taken to accurately define the remanent magnetism direction in each lava. Doell & Cox (1963) suggest that at least six independent specimens from each lava are required for secular variation studies. Such data (Watkins 1965c) from sixteen successive reversely magnetized lavas on Abert Rim, which is a vertical fault scarp 70 miles west of Steens Mountain, show that the secular variation recorded is of

similar magnitude to that observed in North America at present, and in normally magnetized Plio-Pleistocene lavas in Iceland (Wensink 1964). The normal polarity of the initial Steens summit data (Watkins 1963) provided a motive for making a detailed survey of the section, so that a comparison could be made with the data from the reversely magnetized Abert Rim lavas.

Experimental methods

Field

At least six cores of average length 15 cm and 2·5 cm diameter were taken from each lava using a gasoline-powered portable drill. Cores were oriented in geographic co-ordinates while still attached to outcrop: the elevation of the section enabled very long range geographic reference shots to be established, so that orientation of each core was accurate to $\pm 2\frac{1}{2}°$ of arc. The lower limit of the section marks the lower limit of continuous outcrop at a thick scree slope.

Laboratory

From the deepest least-weathered part of each core a specimen of 2·3 cm length was taken for palaeomagnetic measurement. Other specimens were taken for several other studies.

The remanent magnetism was measured using spinner and astatic magnetometers. Unstable components were minimized by treatment in alternating magnetic fields using a triaxial tumbler (Doell & Cox 1967) initially, and a biaxial tumbler (McElhinny 1966) during later stages of the investigation. For the initial detailed examination of magnetic stability in specimens from the lower part of the sampled section (Watkins 1965a), the procedure employed was at that time, conventional: selected specimens from several different lavas were demagnetized in a series of progressively higher alternating magnetic fields of peak values up to 800 Oe to define a coercivity spectrum, which could be used to determine a single field value for application to all specimens. Implicit in this method is the inferrence that the maximum instability is uniform within and between the lavas. Subsequent research (Watkins & Haggerty 1967) has shown that the inherent differential cooling rates in some single lavas may be associated with highly variable magnetic stabilities, and so, clearly, application of a single demagnetizing field to all specimens may result in either an incomplete removal of the unstable component or, in the case of low coercivity components, the addition of spurious components by the demagnetizing process itself (Watkins 1967). This latter possibility is enhanced by the fact that the demagnetizing apparatus was used in the presence of the normal ambient magnetic field which may increase the possibility of adding an anhysteritic component to the remanent magnetism (Patton & Fitch 1962). It is therefore considered to be more realistic to determine the mean direction of remanent magnetism for each lava using the following method: at least three demagnetizing field treatments are applied to each specimen, and the mean direction is then obtained by using one value from each specimen so that a minimum scatter is obtained. The original (untreated) directions were not used, since large unstable components could conceivably create a very close group of directions which are nevertheless not those due to the original magnetic field direction. This procedure was applied, using a computer program, to the 280 specimens taken from lavas 1–42 (ordinate of Fig. 4). The earlier data (lavas 43–71) were recomputed using the same procedure, although not all of these specimens were treated in alternating magnetic fields other than a single 200 Oe value.

Polished thin sections from four different cores in each lava were examined using a Reichert Zetopan-pol reflection microscope with oil immersion and magnifications up to × 2000. The oxidation index of each thin section has been determined. This is a parameter describing the high temperature oxidation state of the titano-

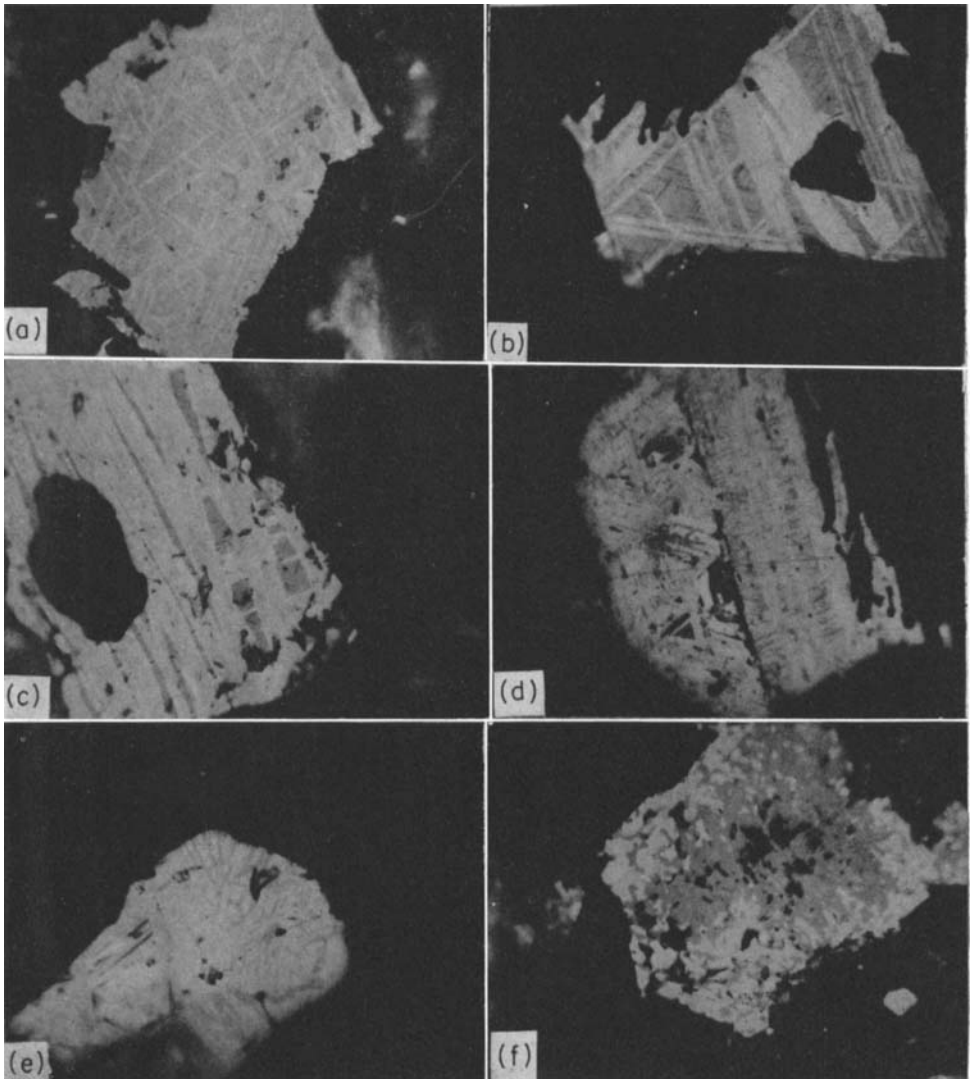

FIG. 1. Reflected light photomicrographs showing the progressive high temperature oxidation of titanomagnetite and its derivatives. All fields of view are 100×130 microns. Silicates are non-reflecting and appear black. For discussion of oxidation indices see text. (a) Titanomagnetite with titanohematite to metailmenite lamellae after ilmenite (light grey). Oxidation index III; from Core 29–2. (b) Triangular and rhomohedral areas of dark grey cubic host material (ilmenite poor titanomagnetite?). The original ilmenite lamellae have now been completely transformed into the light grey lamellae and laths of rutile-titanohematite intergrowths. Some exsolved alumino-spinels exist along the 110 cube faces of the host material. Oxidation index V; from core 39–7. (c) As in previous photomicrograph, except that the dark grey host material is now almost completely replaced by the laths of rutile-titanomagnetite intergrowths. Oxidation index V; from core 38–5. (d) The process shown in the previous two photomicrographs is nearly complete: the dark grey host is completely given over to rutile-titanohematite intergrowths which still retain outlines of the parent laths. An irregular incipient development of pseudobrookite (grey) has appeared (left-centre of photomicrograph). Oxidation index V; from core 39–7. (e) An alternate form of rutile: medium grey sigmoidal rhombs or laths in titanohematite (light grey). Oxidation index V; from core 8–2. (f) Irregular development of pseudobrookite (dark grey) in titanohematite (white). Oxidation index V; from core 10–7.

[*Facing page* 124

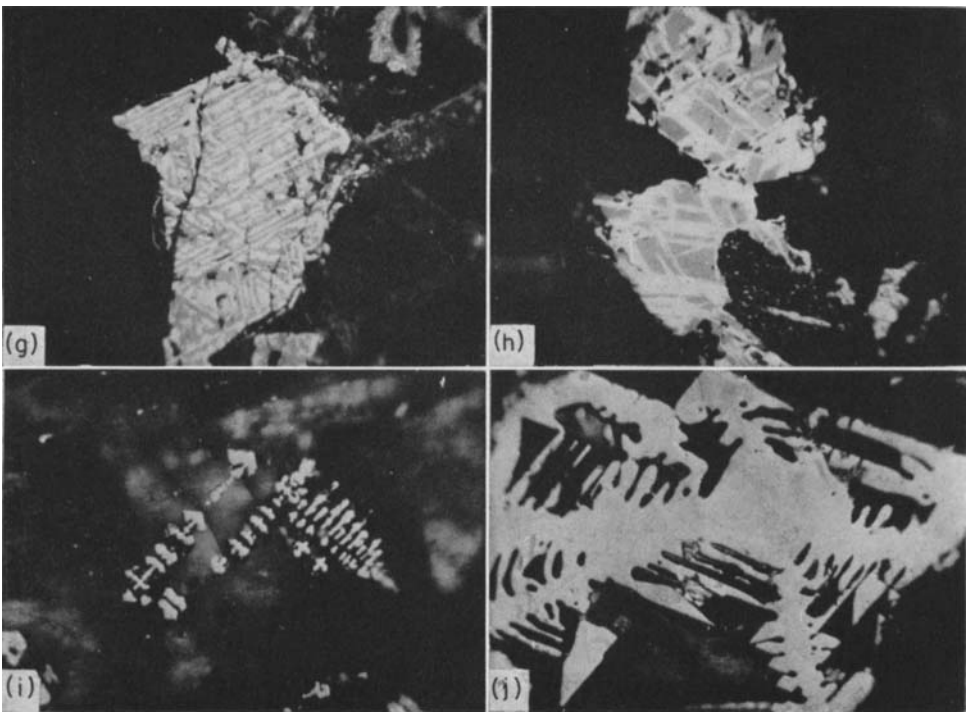

FIG. 1 (*continued*). (g) Irregular lamellae of pseudobrookite (dark grey) after ilmenite in titanohematite after titanomagnetite. Oxidation index V; from core 56–4. (h) Unusual development of titanohematite lamellae in a pseudobrookite (?) host. Oxidation index V; from core 40–3. (i) Apparently quenched titanomagnetite or ilmenite grain, with frond-like habit. Indeterminate oxidation index from core 37–6. (j) Another example of arrested growth, but in a much larger optically homogeneous titanomagnetite grain. Oxidation index I from core 37–6.

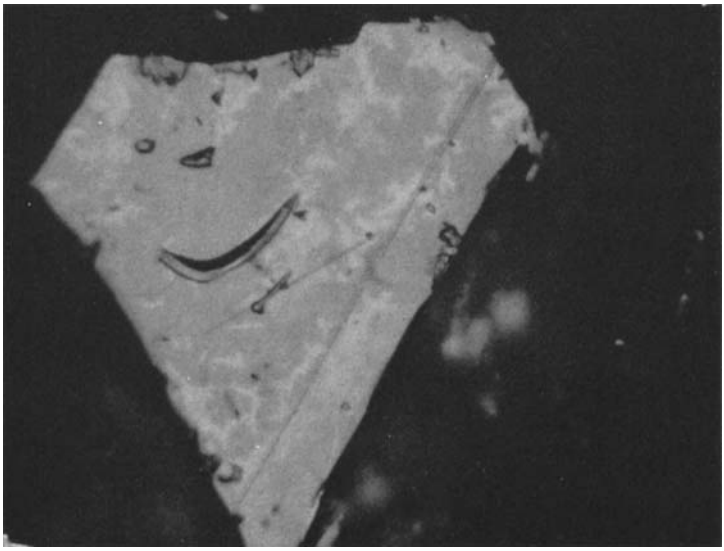

FIG. 2. Fine vermicular replacement of optically homogeneous titanomagnetite (grey) of oxidation index I, by titanomaghemite (light grey). From core 34–1. Field of view is 100×130 microns.

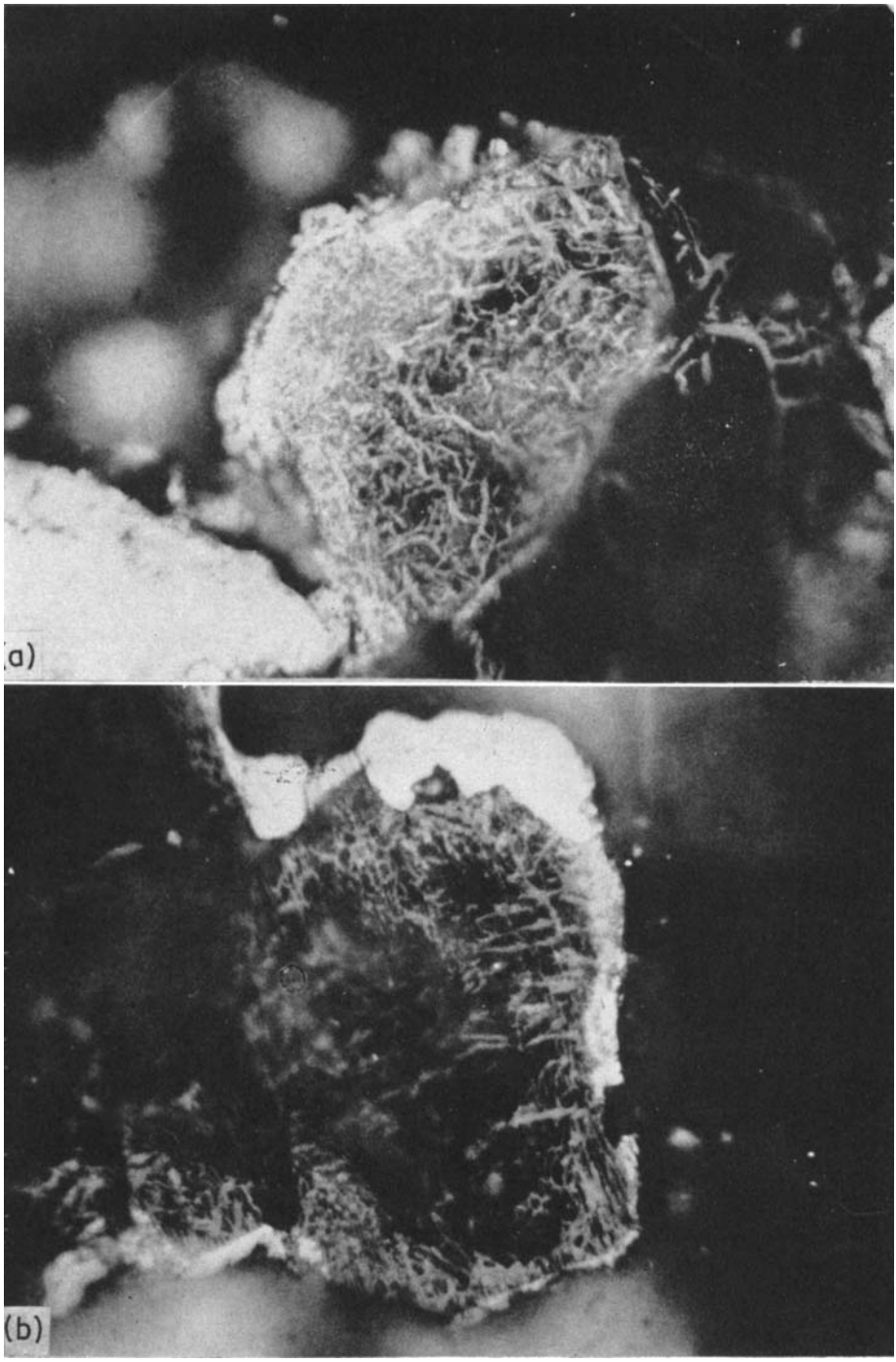

FIG. 8. Reflected light photomicrographs showing secondary iron–titanium oxide in olivine. (a) Web-like development of irregular secondary magnetite (light grey) in olivine, with definite increase in density of intergrowth towards the outer part of the grain where beads of hematite (white) have grown. Hematite grain (white) on bottom left-hand side of the photomicrograph. (b) Fine hematite (white) rim around olivine, increasing in width at upper-centre of photograph, giving way to webs of magnetite (grey) which show crystallographically controlled development, and to the central relatively unoxidized parts of the olivine grain (non-reflecting). Field of view 100×130 microns, both photomicrographs from core 12–4.

magnetites according to the following progressive scheme of indices (Wilson & Watkins 1967):

I: Homogeneous titanomagnetite grains. Colour is light tan.

II: A few ilmenite lamellae may appear in some or all of the titanomagnetite grains, and may be of any width.

III: The titanomagnetite grain is crowded with ilmenite lamellae. The silicates show some reddening.

IV: The sharp, well-defined ilmenite lamellae of III become mottled and distinctly light in colour (Fig. 1(a)). The submicroscopic and heterogeneous nature of the inversion products at this oxidation stage may not permit identification of individual mineral phases, and is best termed ' metailmenite ' (Buddington & Lindsley 1964, p. 326).

V: The original titanomagnetite is now characterized by either rutile or pseudobrookite. Rutile appears either as intergrowths with hematite in thick laths (Fig. 1(b)–(d), or as sigmoidal rhombs in hematite (Fig. 1(e)). The laths occur frequently between relic areas of a dark brown cubic host in which exsolution rods of alumino-spinel exist along 110 faces (Fig. 1(b), (c)). Smith (1968) has used electron probe analyses to show that this characteristic cubic host may not be titanomagnetite, as previously suspected (Wilson & Watkins 1967), but is similar in composition to pseudobrookite which is, however, not cubic. Pseudobrookite occurs as an irregular intergrowth with hematite (Fig. 1(f)), as crystallographically oriented laths intergrowth with hematite, (Fig. 1(g)) or, rarely, as what appears to be host to sharply defined hematite lamellae (Fig. 1(h)). Optical identification of these phases has been supplemented by microsampling and X-ray methods (Watkins & Haggerty 1967) and electron probe methods (Smith 1968).

Discrete grains of ilmenite are similarly affected and also produce as an end product complete pseudomorphs of pseudobrookite with minor subgraphic intergrowths of rutile and titanohematite.

The average oxidation index of a specimen is estimated by scanning about 300 grains. An indeterminable index would be one in which grains of widely variable oxidation index occur, or when the grain size is too small for recognition of the phase involved. This is most often the case in examples of fine quenched material (Fig. 1(i)) although arrested growth is also seen in large grains (Fig. 1(j)). The indeterminable index is of experimental value: it cannot result from the counting and computation method of Wilson *et al.* (1968) in which all observed grains are used to arrive at an ' oxidation number ', meaning that a rare (but not impossible) combination of very high and very low oxidation states in one sample would not be numerically distinguishable from a uniformly moderately oxidized sample. This would obscure relationships between oxidation and any parameter critically dependent on the presence of extreme oxidation states. The average grain size of the largest 30 or so titanomagnetite grains in each section has also been estimated. Maghemite appears to be a low temperature product, and is sometimes seen superimposed on the lower oxidation indices (Fig. 2). If present above about ten per cent of the total surface area of the titanomagnetites, the suffix ' M ' is added to the index.

Curie points were determined using a modified Chevallier balance (Ade-Hall *et al.* 1965), in which the specimen of mass approximately 100 mg is heated rapidly to mask chemical changes which may occur during the process. This was carried out for specimens from the four cores in each lava between numbers 43 to 71 which were examined in polished thin section.

Summary of preliminary and independent results from the Steens Mountain palaeomagnetic collection

Preliminary examination of the remanent magnetism from the collection showed that a polarity change was recorded by the section, and so the oldest 28 lavas in the section which are involved in defining the transition, were examined in detail (Watkins 1965a). Strangway & Larson (1965) also reported the existence of this transition by implication since they describe an upper section of normal polarity overlying reversely magnetized lavas on Steens Mountain. Wilson & Watkins (1967) found a correlation between higher oxidation state of the titanomagnetites and dominance of reversed polarity in the oldest 28 lavas in the section. Although the significance of this correlation is far from clear (Larson & Strangway, 1968; Wilson 1968; Watkins 1968b) there is little doubt that the data represent a true geomagnetic polarity transition. This conclusion is strongly supported by the palaeointensity estimate obtained by Coe (1967) using specimens from lava number 56, which indicates that lava cooled in a geomagnetic field of 0·11 G, or less than one quarter of the present field intensity, as might be expected during a polarity transition (Rikitake 1965, p. 81). Goldstein *et al.* (1968) have recently verified this result, and extended the observations across the polarity transition: they obtained results corresponding to a systematic decrease in palaeointensity from 0·5 G either side of the central part of the transition, to 0·025 G in the central part. Prevot & Watkins (1969) have, however, obtained a palaeointensity of 0·6 G from lava 57, suggesting that the transition might not have been a smooth decrease of intensity through a minimum, and later increase. Baksi *et al.* (1967), in showing that the polarity transition took place $15{\cdot}1 \pm 0{\cdot}3$ million years

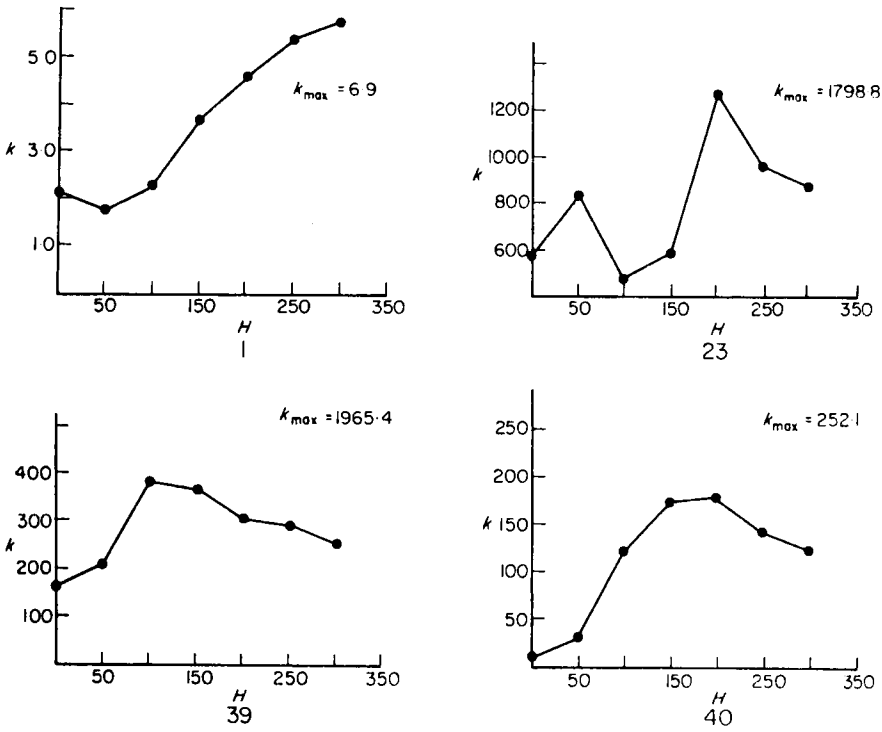

FIG. 3. Variation of the precision parameter k (Fisher 1953) for the directions of remanent magnetism in four lavas, as a function of the peak alternating demagnetizing field (H), in oersteds. For the stratigraphic position and number of specimens in each lava, see Table 1. For the explanation of the meaning and method of computation of k_{max}, see text.

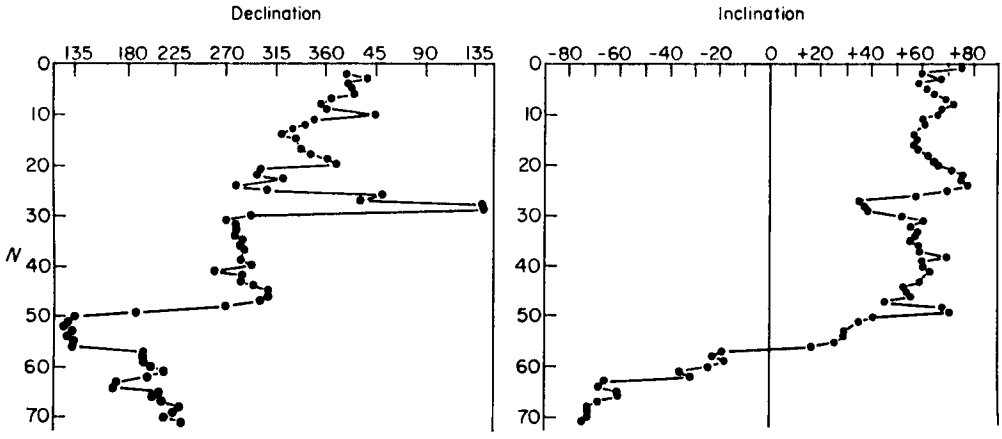

FIG. 4. Mean declination and inclination of remanent magnetism following demagnetization for each lava, as a function of stratigraphic position. N = number of lava in the section: increasing number corresponds to increasing age. Declination is in degrees east of geographic north. Inclination is in degrees with respect to the horizontal: positive is below horizontal: negative is above horizontal.

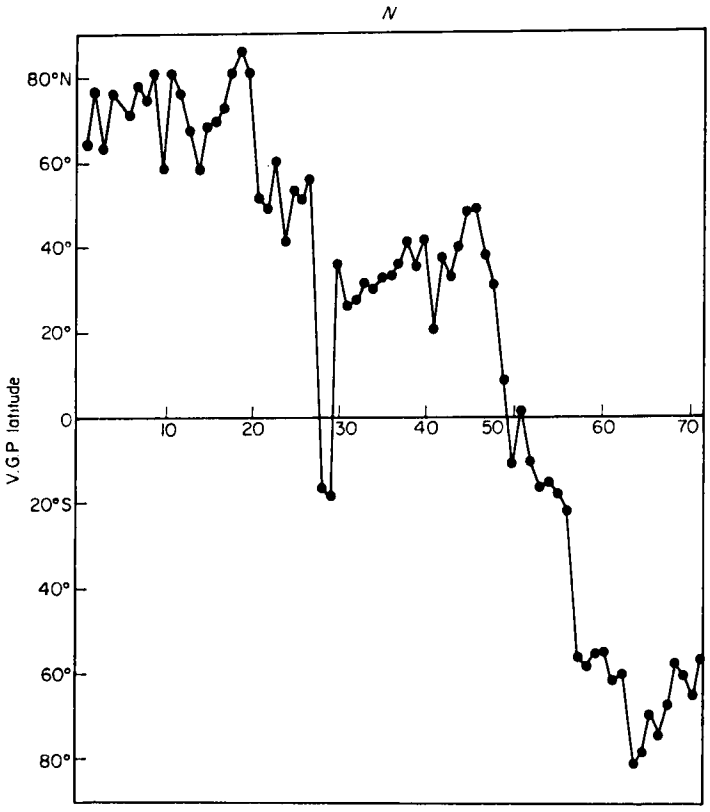

FIG. 5. The latitude of the virtual geomagnetic pole for each lava. Absissa is number of lava, increasing with increasing age. For the number of specimens per lava and the results of the alternating magnetic field treatments, see Table 1.

ago, have noted that no detectable K: Ar age difference exists across the entire sampled section.

The relevance of these results to final analysis of the palaeomagnetic data from the entire section will be demonstrated below.

Results

Unstable components

Fig. 3 shows the results of progressive demagnetization of all specimens from four different lavas. The Fisher (1953) parameter k is shown as a function of the demagnetizing field value (H). Also included in each diagram is the k_{max} value, which corresponds to the minimum scatter value obtained using one direction of remanent magnetism from each treated specimen. Table 1 shows the k_{max} and the k values for each lava at each H value.

Remanent magnetism

The declination and inclination of remanent magnetism for each lava, corresponding to the least scatter computation as discussed above is given in Table 1. The correction for geological dip has been linearly distributed across lavas 1 to 40 where the 11° maximum dip diminishes to 0°. Fig. 4 shows the declination and inclination of remanent magnetism as a function of stratigraphic position. The latitude of the virtual geomagnetic pole for each lava is similarly presented in Fig. 5. The relevant Fisher (1953) statistical parameters are given in Table 1.

Opaque mineralogy

The oxidation index and the average size of the 30 or so largest titanomagnetite (or derivative) grains for each of four randomly selected specimens from each lava are given in Table 2. Fig. 6 shows the distribution of the oxidation indices.

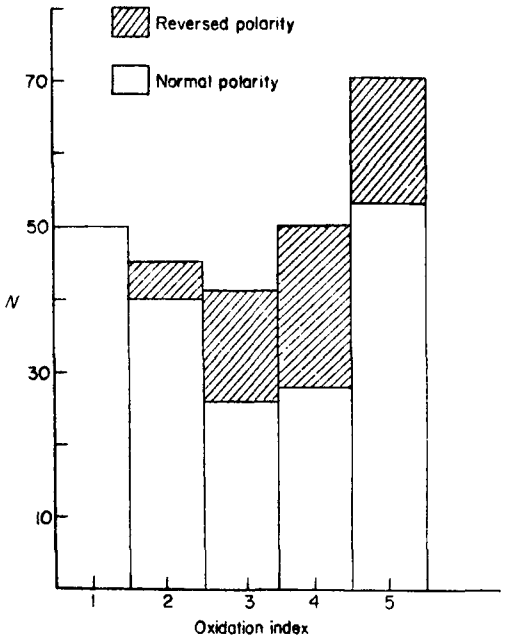

FIG. 6. Histogram showing the distribution of the optically defined high temperature oxidation indices. N = number of occurrences. For explanation of oxidation index see text. Data from reversely magnetized lavas shaded.

Curie points

The Curie point data for lavas 43 to 71 have been published elsewhere (Wilson & Watkins 1967) and are not repeated here.

Discussion

Fig. 3 shows clearly that in the four lavas examined no one demagnetizing field value (H) will result in peak k values or minimum scatter of remanent magnetism directions for every lava. This supports the validity of the preferred method used in computing the mean direction of remanent magnetism for each lava, which is based on the assumption that stability differences exist within each lava, and therefore different specimens within any lava may require different peak demagnetizing field values to arrive at the most meaningful mean direction for a given lava.

The most striking feature of the remanent magnetism directions (Fig. 4) is the well-defined transition of inclination from 70° up to 70° down. This corresponds to a northerly migration of the virtual geomagnetic pole (Fig. 5). The significance of these data can be discussed in the following seven sections.

1. *Validity of transition*

The oxidation states of the titanomagnetites (Table 2, Figs 1 and 6) are of a wide range both within and between lavas. As presented elsewhere (Wilson & Watkins 1967) there is a tendency for low Curie points, when they exist, to be associated with low oxidation states. Pseudobrookite (Fig. 1(f) and (g)) which is stable below 585 °C (Lindsley 1965) occurs in several lavas, being diagnostic of oxidation index V (Table 2). None of the samples lavas are close to known thermal sources and so no significant reheating has occurred. These facts, together with the great but non-systematic variability in oxidation state, intensity of magnetization, and stability, and the generally regular variation in the remanent magnetism directions exclude the possibility that the remanent magnetism directions are a function of petrological properties and not the original ambient geomagnetic field.

The oxidation state data (Table 2 and Fig. 6) are also relevant to the enigma of the meaning of observed correlations between higher oxidation states and dominance of reversed magnetic polarity in basalts (summary by Watkins & Haggerty 1968, Bullard 1968). Since the oxidation indices of the lavas of normal polarity, which constitute the younger 56 of the 71 successive lavas, are almost uniformly distributed across the oxidation spectrum, the data therefore show that lavas of normal polarity are not preferentially associated with lower oxidation states. Only the distribution of the oxidation indices of the reversely magnetized lavas were responsible for the observed strong correlation between oxidation index and percentage of reversely magnetized specimens in lavas 43 to 71 (Wilson & Watkins 1967) which is still apparent although far less perfect, if the data for the entire section are similarly processed following normalizing to provide equal weight for normal and reversely magnetized lavas.

It is suggested that the oxidation variation shown in Table 2 and Fig. 6 is evidence against the possibility of meaningful resolution of the previously observed correlation (discussed above) in terms other than a function of sampling. It would appear that a major and perhaps terminal difficulty in studies of oxidation and polarity relationships as originally suggested by Blackett (1962), is the collection of specimens. Within and between-lava oxidation variations virtually eliminate, at this time, the prospects of formulating a meaningful model, which is far too sensitively involved with the numerous factors determining the exact nature of the sample collection from outcrop to be clearly and meaningfully related to any phenomena causing higher oxidation during periods of reversed polarity.

Table 1

Steens Mountain palaeomagnetic data

Lava number	N	D	I	K_0	K_{100}	K_{200}	K_{max}	α_{95}	θ_{63}	θ'	ϕ'
1	6	332·9	+75·7	2·1	2·2	4·6	7·0	27·35	31·02	64·4	212·9
2	7	17·8	+60·5	4·4	4·3	4·4	4·8	30·85	37·63	76·7	330·9
3	7	37·8	+67·8	793·4	435·8	632·9	866·3	2·05	2·75	63·2	300·8
4	7	18·0	+58·9	36·6	47·9	44·7	49·3	8·68	11·53	76·1	338·2
5	6	21·8	+62·5	134·6	262·7	505·8	532·1	2·91	3·50	74·2	320·0
6	6	5·1	+69·9	195·0	137·3	185·3	188·4	4·89	5·89	78·3	256·6
7	6	25·8	+65·2	346·7	295·7	350·7	393·8	3·38	4·07	71·3	308·7
8	7	255·5	+72·7	19·7	24·1	24·5	25·6	12·15	16·01	74·4	232·7
9	6	0·4	+68·2	476·9	493·8	479·6	597·8	2·74	3·31	81·3	243·0
10	6	44·9	+66·4	41·5	95·7	141·6	242·3	4·31	5·19	58·6	304·4
11	7	348·2	+60·4	65·0	193·6	151·7	376·1	3·12	4·17	81·1	146·5
12	6	241·5	+61·0	6·9	143·2	91·7	171·0	5·14	6·18	76·3	155·1
13	6	330·4	+58·9	184·6	108·2	133·2	140·1	5·68	6·83	67·6	153·8
14	6	319·2	+56·8	11·1	12·6	10·9	13·5	18·89	22·10	58·6	155·8
15	7	331·9	+58·4	321·9	383·5	790·4	701·7	2·28	3·05	68·6	151·5
16	7	334·0	+57·0	546·8	376·9	378·2	612·7	2·44	3·26	69·5	145·7
17	6	336·9	+58·8	65·4	259·4	522·1	653·1	2·62	3·16	72·4	149·2
18	7	347·6	+62·4	19·2	87·4	275·9	400·1	3·02	4·04	80·9	161·9
19	7	0·6	+64·4	11·9	19·9	38·1	39·6	9·72	12·87	86·4	248·3
20	6	9·3	+66·5	8·1	8·2	8·8	9·2	23·39	26·95	81·0	284·1
21	7	302·0	+74·2	153·8	406·6	185·1	602·9	2·46	3·29	51·5	199·3
22	7	297·0	+76·2	285·0	264·2	545·6	623·4	2·42	3·24	49·1	204·7
23	6	322·3	+75·4	476·7	479·5	1257·5	1798·8	1·58	1·91	60·4	206·6
24	6	276·8	+78·4	25·1	36·2	25·7	40·9	12·10	12·65	41·3	211·3
25	6	306·1	+70·5	164·4	232·5	578·4	648·9	2·63	3·17	53·5	189·7
26	6	52·0	+57·7	6·2	9·2	7·4	9·3	23·24	26·79	50·8	319·8
27	7	28·8	+35·4	23·9	285·3	33·3	450·6	2·85	2·67	56·5	6·2
28	6	140·0	+37·4	144·8	350·2	532·8	932·5	2·20	5·12	−16·5	280·2
29	6	146·6	+39·0	146·1	119·4	73·5	130·8	5·88	7·13	−18·3	274·0
30	6	291·5	+52·3	26·5	23·5	25·4	25·5	13·52	4·23	36·5	165·2
31	6	268·9	+60·6	3·9	5·0	8·2	8·5	24·36	2·80	26·1	185·2
32	6	275·5	+55·9	52·7	584·6	337·3	916·8	2·21	5·30	27·4	177·2
33	6	279·0	+58·3	319·1	222·9	149·0	249·7	4·25	24·22	31·1	177·9
34	6	278·4	+57·8	31·4	40·2	125·6	128·8	5·93	1·82	30·4	177·6
35	7	283·2	+55·8	135·0	278·6	243·2	364·3	3·17	5·09	32·5	173·1
36	8	282·5	+58·5	143·2	203·2	831·4	831·5	1·92	48·92	33·5	176·4
37	7	285·3	+59·1	33·6	103·2	140·4	232·2	3·97	4·99	35·7	175·7
38	7	284·3	+70·6	12·2	10·7	10·8	11·3	18·7	5·83	41·6	193·4
39	6	283·8	+60·5	163·6	381·7	304·6	1965·4	1·51	15·25	35·7	178·3

Table 1 (*continued*)

Lava number	N	D	I	K_0	K_{100}	K_{200}	K_{max}	α_{95}	θ_{63}	θ'	ϕ'
40	6	293·0	+60·4	9·7	120·0	172·9	252·1	4·23	15·37	41·6	174·0
41	6	256·9	+62·6	1·5	2·2	2·9	2·9	48·19	6·78	20·6	193·0
42	6	287·5	+60·2	38·1	122·2	257·2	262·5	4·14	7·75	37·8	176·2
43	6	285·1	+58·6	67·0	—	121·9	121·9	4·84	25·52	35·3	175·3
44	6	293·0	+52·4	5·5	—	28·6	28·6	12·82	35·05	37·6	164·5
45	8	311·0	+55·2	7·0	14·1	24·6	27·8	10·69	17·68	51·9	157·8
46	6	307·6	+55·2	204·9	—	142·4	142·4	5·64	5·90	49·4	159·8
47	7	298·8	+45·4	71·0	—	846·4	184·4	5·81	16·58	38·5	154·5
48	6	267·5	+67·5	4·3	20·7	23·1	28·0	22·04	7·17	29·5	195·2
49	6	156·3	+72·0	2·7	4·5	2·3	5·5	31·47	6·80	11·6	254·4
50	7	133·4	+40·7	22·4	—	20·1	20·1	13·46	13·99	−11·3	284·4
51	6	124·5	+39·6	5·4	83·6	11·7	187·4	4·91	7·31	− 7·2	291·6
52	6	123·7	+38·0	24·1	—	19·1	19·1	13·98	10·73	− 7·6	292·9
53	7	128·7	+36·9	59·0	64·9	83·6	127·1	5·37	7·17	−11·1	289·6
54	7	130·0	+32·9	10·8	—	26·6	260·6	5·09	6·80	−13·9	290·2
55	6	129·8	+29·2	13·2	—	136·6	136·6	5·74	13·99	−15·7	291·7
56	6	131·2	+17·1	12·8	—	52·4	52·4	6·08	7·31	−22·1	294·8
57	6	195·1	−20·8	53·7	—	40·4	40·4	8·96	10·73	−55·4	214·7
58	6	194·6	−23·7	32·0	—	166·7	166·7	4·92	5·92	−57·2	214·5
59	7	194·7	−18·2	185·0	—	104·5	104·5	4·48	5·98	−54·3	216·1
60	7	202·5	−24·9	3·0	—	37·2	37·2	9·84	13·04	−54·6	201·6
61	7	213·5	−35·1	3·8	10·9	15·8	16·9	15·11	19·74	−53·4	180·7
62	7	199·3	−31·9	32·2	—	29·4	29·4	11·23	14·83	−59·8	202·7
63	7	170·6	−66·1	91·8	47·6	93·9	95·1	6·22	8·29	−81·2	16·1
64	6	169·2	−68·7	72·6	843·2	12·5	3716·0	3·48	4·19	−78·1	27·6
65	6	209·5	−61·0	166·0	—	1613·0	1613·0	2·14	2·58	−68·3	143·0
66	6	201·9	−60·5	500·3	—	757·6	757·6	2·49	3·00	−73·8	148·3
67	8	211·1	−69·3	220·0	—	273·4	273·4	3·66	5·33	−67·0	114·4
68	6	228·5	−72·8	375·0	425·3	149·7	627·7	2·68	3·23	−56·4	106·8
69	8	221·4	−72·9	700·0	—	362·7	362·7	2·91	4·24	−60·1	105·6
70	6	212·9	−73·2	156·0	—	375·8	375·9	3·50	4·21	−64·1	101·5
71	7	229·9	−75·3	103·0	—	495·9	495·9	3·09	4·13	−55·1	100·0

Lava numbers are in stratigraphic order, with the larger number corresponding to the older lava. N = number of cores per lava. D and I are declination and inclination of mean remanent magnetism in each lava, following minimizing of unstable components. D is in degrees east of north. I is with respect to horizontal; downwards, is positive and upwards, is negative. K is Fisher (1953) precision parameter; suffixes 0, 100 and 200 are the demagnetizing field value applied. K_{max} is the precision parameter obtained by a minimum scatter criterion (see text). α_{95} = semi-vertical angle of 95 per cent confidence cone. θ_{63} = circular standard deviation. θ' and ϕ' are latitude and longitude of the virtual geomagnetic pole: θ' is in degrees east of Greenwich; ϕ' is positive when in northern hemisphere, and negative in southern hemisphere.

Table 2

Optically-defined high temperature oxidation index of the titanomagnetites, and grain size average

Specimen number	Oxidation index	Average size (μ)	Specimen number	Oxidation index	Average size (μ)	Specimen number	Oxidation index	Average size (μ)
1–2	IIM	30	2–3	IIM	60	3–3	?	5
1–3	IIM	20	2–4	?	30	3–4	?	5
1–4	I	30	2–5	I	5	3–5	?	40
1–5	?	30	2–6	VI	40	3–7	IV	40
4–1	IV	20	5–1	V	30	6–1	IV	40
4–4	IV	30	5–2	V	30	6–3	?	40
4–6	V	40	5–3	V	40	6–4	IV	60
4–7	V	15	5–4	V	20	6–6	II	80
7–1	V	15	8–1	?	60	9–2	I	60
7–2	IIM	10	8–3	V	80	9–5	V	80
7–4	V	40	8–4	II	100	9–6	IV	80
7–6	V	40	8–6	II	60	9–7	IIII	60
10–1	V	80	11–1	I	40	12–2	II	40
10–2	?	60	11–2	II	30	12–3	II	40
10–3	III	40	11–3	III	40	12–4	V	50
10–4	III	50	11–4	III	30	12–5	?	40
13–1	?	30	14–1	V	30	15–1	II	40
13–3	IV	30	14–3	I	10	15–2	II	40
13–5	V	40	14–5	II	20	15–5	?	40
13–6	V	60	14–6	V	40	15–6	III	40
16–1	I	20	17–1	V	40	18–1	?	3
16–2	?	40	17–2	?	40	18–2	II	5
16–3	I	20	17–3	V	40	18–3	V	40
16–4	IV	40	17–5	V	40	18–7	V	50
19–2	II	50	20–1	V	30	21–1	II	20
19–4	II	60	20–2	?	40	21–2	I	10
19–5	?	60	20–3	IV	40	21–3	I	10
19–6	II	60	20–5	V	30	21–4	I	10
22–1	I	10	23–1	V	30	24–1	I	20
22–3	?	30	23–2	V	30	24–2	I	15
22–5	?	20	23–3	V	30	24–3	I	10
22–6	I	20	23–4	?	30	24–6	II	20
25–2	I	80	26–1	I	40	27–1	I	15
25–3	II	100	26–2	I	40	27–2	II	40
25–4	I	60	26–4	I	60	27–5	I	40
25–7	II	60	26–6	III	80	27–8	?	10
28–1	V	40	29–1	V	40	30–1	II	60
28–2	V	40	29–2	IV	60	30–2	II	60
28–3	V	40	29–3	IV	60	30–3	?	60
28–4	V	60	29–4	V	60	30–4	?	40
28–5	V	60	29–5	IV	60	30–5	?	40
28–6	V	60	29–6	IV	60	30–6	?	60
31–2	I	60	32–2	II	80	33–1	II	60
31–3	?	20	32–3	II	100	33–3	I	100
31–5	I	80	32–4	I	100	33–4	I	100
31–6	I	60	32–6	I	80	33–6	I	80
34–1	IM	80	35–1	I	60	36–1	I	100
34–2	IM	80	35–4	I	80	36–2	I	100
34–3	I	60	35–6	I	80	36–3	I	80
34–4	IM	80	35–7	I	60	36–4	I	80

Table 2 (*continued*)

Specimen number	Oxidation index	Average size (μ)	Specimen number	Oxidation index	Average size (μ)	Specimen number	Oxidation index	Average size (μ)
37–4	I	80	38–4	?	60	39–3	IV	80
37–5	I	100	38–5	V	80	39–4	V	80
37–6	I	80	38–6	?	60	39–5	V	60
37–7	I	80	38–7	?	80	39–7	V	80
40–1	V	60	41–1	V	60	42–1	?	60
40–2	?	80	41–3	V	60	42–2	I	100
40–3	V	60	41–4	V	60	42–3	?	80
40–6	V	80	41–5	V	60	42–6	V	60
43–1	IV		44–1	IV		45–2	I	
43–2	IV		44–2	III		45–3	II	
43–4	IV		44–4	III		45–6	II	
43–5	IV		44–6	II		45–8	II	
46–1	IV		47–1	?		48–1	III	
46–4	III		47–3	V		48–3	III	
46–5	III		47–5	IV		48–4	III	
46–6	IV		47–6	?		48–6	IV	
49–1	III		50–1	III		51–1	II	
49–2	IV		50–2	II		51–2	I	
49–4	I		50–3	II		51–4	II	
49–6	III		50–6	III		51–6	III	
52–1	?		53–1	IV		54–1	I	
52–2	IV		53–2	III		54–2	II	
52–3	V		53–4	II		54–3	I	
52–4	IV		53–5	V		54–7	III	
55–2	II		56–1	III		57–1	V	
55–3	II		56–3	II		57–2	V	
55–4	II		56–5	?		57–5	V	
55–6	II		56–6	III		57–6	V	
58–1	V		59–2	V		60–2	III	
58–3	V		59–3	V		60–3	III	
58–5	V		59–4	V		60–4	III	
58–6	V		59–7	IV		60–7	III	
61–1	II		62–3	V		63–1	V	
61–3	IV		62–4	III		63–4	IV	
61–5	II		62–5	IV		63–5	III	
61–6	II		62–6	V		63–6	V	
64–1	IV		65–1	?		66–1	IV	
64–2	V		65–2	II		66–3	III	
64–4	IV		65–4	III		66–4	III	
64–6	IV		65–6	V		66–6	IV	
67–1	IV		68–1	IV		69–1	III	
67–3	IV		68–2	III		69–4	III	
67–5	III		68–4	III		69–7	IV	
67–8	III		68–6	IV		69–8	III	
70–1	IV		71–1	IV				
70–3	IV		71–4	IV				
70–4	IV		71–6	IV				
70–6	IV		71–7	IV				

Specimen number: first number is lava (ordinate of Fig. 4); second number refers to the core.

Oxidation index: see text.

Average size: this is the average size of the largest thirty or so titanomagnetite grains.

2. *Lava extrusion history*

Throughout the following analyses, the assumption will be made that the Steens Mountain lavas as sampled were extruded in fairly regular succession. As pointed out earlier, no field evidence exists to cast definite doubt on this assumption, but the possibility that the section is composed of a series of volcanic pulses separated by periods of inactivity cannot be absolutely precluded. Such events would be very relevant to the analyses to be presented.

Fig. 7 illustrates an attempt to discover if there exists any evidence in the relationship of the successive remanent magnetism directions to indicate time breaks in the section. The accumulated angular difference between the successive mean remanent magnetism directions for the 71 lavas are plotted as a function of stratigraphic position. Also included in the diagram is an indication of the virtual geomagnetic pole (V.G.P.) latitude as a function of stratigraphic position: the horizontal bar is clear for V.G.P. latitudes equatorward of 30°, and is solid for V.G.P. latitudes higher than 30°.

It can be seen that with three major and some minor exceptions the accumulative curve in Fig. 7 is linear. The linear segments are consistent with broadly regular intervals between lavas superimposed on a regularly moving ambient geomagnetic field. It is impossible to accept the alternative interpretation requiring rapidly varying geomagnetic field movement, and complementary pulsing volcanic activity.

The three major departures from linearity in the accumulative curve at lavas 27 to 33, 47 to 50, and 55 to 57, correlate closely with the low latitude V.G.P. positions associated with the beginning and end of the major segment of the polarity transition, and with a short departure of the V.G.P. to equatorial regions in the later stages of the transition (Fig. 5). It is suggested that the breaks in the curve correspond, then, to geomagnetic field behaviour probably associated with a change in the relative contribution of the non-dipole to dipole component, rather than being due to major time breaks in the lava extrusion pattern during a period of regular ambient geomagnetic field movement. This does not in itself exclude the possibility of time breaks in the lava extrusion history of the Steens scarp, since the ambient magnetic field movement is somewhat cyclic and could conceivably result in repetition of remanent magnetism directions following hiatuses, but it is suggested that such

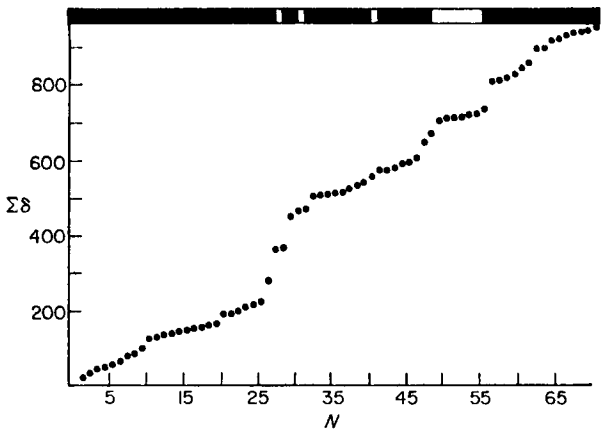

FIG. 7. The accumulative angular difference in the directions of mean remanent magnetism (δ) between successive lavas (*N*) in degrees. *N* is the stratigraphic position of the lava, increasing in number with increase in age. The horizontal bar at the top of the diagram indicates the latitude of the virtual geomagnetic pole calculated from the natural remanent magnetism of each lava (*N*): clear represents a latitude of 30° or less; solid is a latitude above 30°.

breaks are most probably not very large relative to the average time between lavas. If this *were* so, then the effect of dipole wobble or even polar wandering would probably be effective in causing a slope change in Fig. 7 or large angular differences of remanent magnetism directions between lavas extruded before and after such movements, while the V.G.P. remained at higher latitudes. It is concluded that the palaeomagnetic data from Steens Mountain section are consistent with, but do not unequivocally prove, a history which consists of a series of lavas extruded at regular intervals. In other words, a necessary but insufficient condition is satisfied for regular extrusion.

3. *Morphology of the polarity transition*

Figs 4 and 5 show that, except for a sequence of four lavas (26 to 29) a regular movement of the virtual geomagnetic pole has occurred from southern to northern latitudes. The four anomalous lavas diverge very strongly from the general trend, the virtual geomagnetic pole changing from latitude 40° North to southern equatorial latitudes, prior to returning to the higher northern latitudes.

The remanent magnetism of these four lavas is due either to anomalous petrological properties, post-cooling processes, or original geomagnetic field behaviour. The results of polished section examination of the lavas involved, which are included in Table 2, show that they reached very high oxidation states. The index mineral pseudobrookite, which is diagnostic of oxidation index V cannot be formed below 585 °C suggesting that the high oxidation in lavas 26 to 29 is certainly of initial cooling origin. This conclusion is reinforced by the fact that the olivines present exhibit magnetite and hematite symplectics (Fig. 8, facing page 125) which Haggerty & Baker (1967) show are unlikely to form below 800 °C. Watkins & Haggerty (1967, Fig. 16) have shown that such high oxidation states in some olivine basalts are associated with high intensity of magnetizations and high magnetic stability. Lavas 27–29 possess such properties. These facts and the absence of local thermal sources lead to the conclusion that the remanent magnetism in the critical lavas is definitely of initial cooling origin. The departure of the remanent magnetism directions in these lavas compared to those in the adjacent lavas is so large that magnetic anisotropy (Uyeda *et al.* 1963) cannot be considered relevant. The movement of a virtual geomagnetic pole (V.G.P.) from high latitudes to equatorial latitudes without a polarity change occurring has been observed by Cox (1966) in Alaska, Dagley *et al.* (1967) in Iceland, and most recently by Doell (1968) in Hawaii. By comparison with the data from other Pacific lavas, Cox (1966) attributes his observation to an increase in the relative contribution of the non-dipole component to the observed field. Doell (1968), on the other hand shows that in the case of the lavas with low V.G.P. latitude in Hawaii, the departure path is such that the behaviour is most probably a function of variation in the dipole configuration. There is no particular theoretical reason why a diminishing or equatorial-moving dipole field must be succeeded by a polarity change and not merely a return to the original polarity. Since, as has been discussed in part above and as will be further developed, it is considered highly probable that the Steens Mountain lavas were extruded in rapid succession, it follows that the data are due to a rapid movement of the V.G.P. from northern to equatorial latitudes shortly after a change from southern to northern high latitudes. This change is most easily accounted for by a decrease in dipole contribution to the observed field since the path of the V.G.P. is not along a meridian, and the geomagnetic field rate of movement appears to increase as low latitudes are approached by the V.G.P. Data representing the same polarity transition and later field behaviour recorded on another continent would assist in determining the relative roles of non-dipole and dipole field.

It is unlikely that the proximity in time of the true polarity transition and the low latitude V.G.P. is a coincidence: the implication is that the low latitude V.G.P.

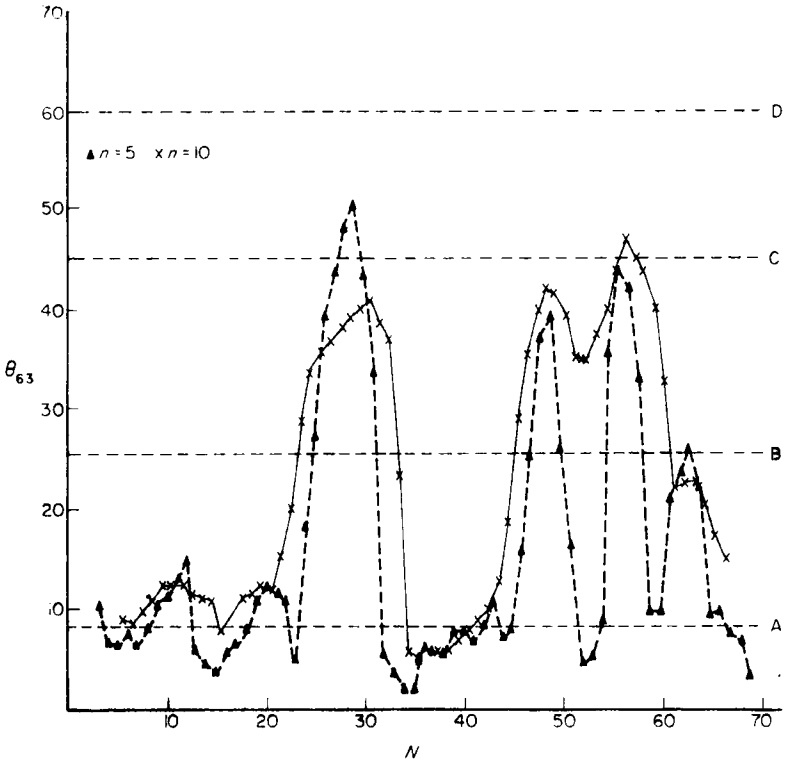

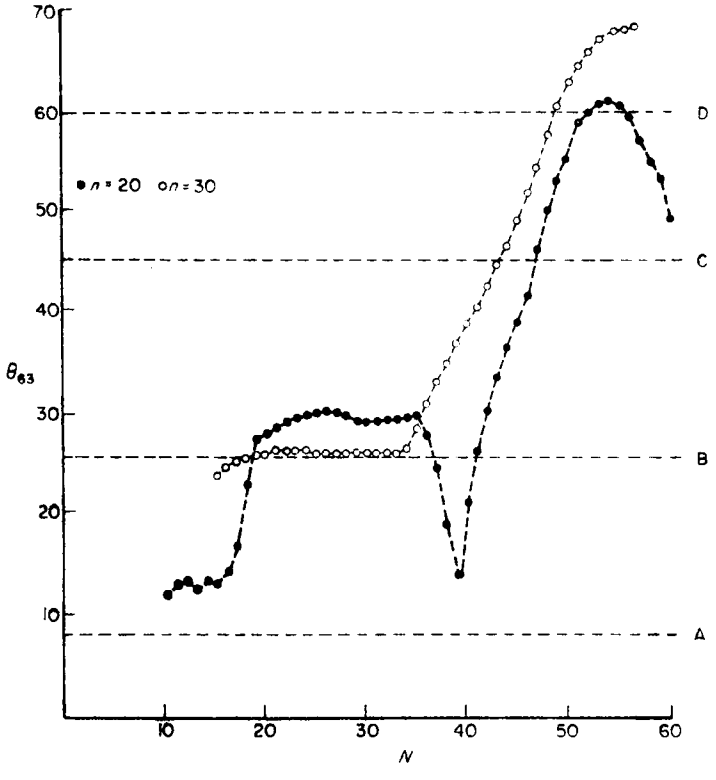

occurred during a period of dipolar instability associated with the final phases of the polarity transition. Together with the fact that Ito & Fuller (1968) have shown almost exactly the same behaviour in their study of a Lower Pliocene polarity transition from reversed to normal polarity, as recorded in a single Oregon pluton, the data may be very relevant indeed to an understanding of some reversal processes. In their study, Ito & Fuller (1968) show a systematic change in inclination from about 60° up (reversed), to 45° down (normal) preceding a systematic decrease in inclination to almost 0° and later return to higher positive values. Although limited, there are clearly sufficient data to suggest that serious consideration might profitably be given to the reality of a ' rebound effect ' during the final stages of at least some polarity transitions. The analogue solutions obtained by Mathews & Gardner (1963) for the output of Rikitake's (1958) double-disk dynamo model of the geomagnetic field are not inconsistent with the observed ' rebound ' described here. The alternate explanation for the data is of course, that the two very similar observations are purely coincidental; but if this is invoked as an explanation, it must be realized that two of only four well-documented palaeomagnetic polarity transitions show this effect (for summary of other transitions studied, see Watkins (1965a)).

4. *Magnitude of the non-dipole component*

An estimate of the relative contribution of the non-dipole component to the total magnetic field can be obtained in terms of an appropriate geomagnetic field model. One such model is that presented by Irving & Ward (1964). It expresses the latitude dependence of the circular standard deviation of magnetic directions, resulting from a rapidly varying non-dipole component superimposed on a steady axial dipole field.

The available palaeointensity results (Coe 1967; Goldstein *et al.* 1968), the variation of the palaeolongitude (Table 1), and the more rapidly moving field (Fig. 7) suggest that the non-dipole field is almost certainly present throughout the transition. This is a necessary requirement for application of the model, which could not legitimately be applied to a purely dipole behaviour. The application of the data to Irving & Ward's (1964) model is shown diagrammatically in Fig. 9. The latitude (λ), the circular standard deviation (θ_{63}), the ratio of the non-dipole field (*Fd*), to the equatorial dipole field intensity (*Fo*) are related by the equation:

$$\theta_{63} = 46{\cdot}8\, Fd/Fo\, [1+3\sin^2\lambda]^{-\frac{1}{2}}.$$

Rigorous application of any palaeomagnetic data to this model requires that the remanent magnetism directions are symmetrically distributed about the mean. As in most palaeomagnetic studies this requirement is not met by the data groups in all cases.

Calculation of θ_{63} is best made from groups of successive lavas, applying unit vector per lava, or point in time. The number of lavas in each group can express the effectiveness of the computation as a means of filtering geomagnetic variations. In order of increasing width, such computational filtering would be effective on non-dipole components of the secular variation; wobbling dipole or random walk

FIG. 9. Variation of the circular standard deviation (θ_{63}) as a function of mean stratigraphic position (lava number) for four different group sizes. N = number of lava: number increases with increasing age. Data points are the θ_{63} values for overlapping groups of n successive lavas: upper diagram shows θ_{63} values for $n = 5$(▲) and 10(×): lower diagram for $n = 20$(●) and 30(○). Successive θ_{63} values are obtained by sliding the respective group limits down the section of lavas: for computation of θ_{63}, data from the adjacent older lava are added, and data from the adjacent younger lava are subtracted. *A* to *D* are four different values of θ_{63} or *Fd*/*Fo* ratios (Table 3) where *Fd* and *Fo* are the magnitude of the non-dipole and equatorial main dipole components respectively (Irving & Ward, 1964). For the limitations of these computations see text: it is emphasized that the computational method produces artificial smoothing. Completely independent θ_{63} values are separated by n data points in each case.

Table 3

Ratio of non-dipole field (Fd) to equatorial dipole field (Fo) corresponding to the four levels of the circular standard deviation (θ_{63}) in Fig. 9

Level	θ_{63}	[Fd/Fo]*	[Fd/Fo]†
A	8	0·27	0·29
B	25	0·83	0·90
C	45	1·51	1·62
D	60	1·98	2·16

* When the palaeolatitude (λ) = the present Steens Mountain latitudes of 42° 40′ North.

† When $\lambda = 51° 30'$. This is obtained from the virtual geomagnetic pole position of 80° North, 220° East resulting from the original Steens Mountain palaeomagnetic survey (Watkins 1965b). The mean Miocene pole of 165° East, 77° North obtained by Doell & Cox (1961, p. 256) provides a value of λ of 43·5°, or close to the present latitude.

All values of *Fd/Fo* are obtained from: $\theta_{63} = 64{\cdot}8\, Fd/Fo(1+3\sin^2\lambda)^{-\frac{1}{2}}$ (Irving & Ward 1964).

of the dipole; and large scale polar wandering. Fig. 9 shows the results of applying a sliding filter groups of $n = 5$, 10, 20, and 30 successive lavas. The term ' sliding filter ' refers to the method of obtaining successive values of θ_{63} which is essentially a vectorial version of the ' moving average ' technique: to obtain successive points, a data point from above is added, and a data point from below the given group is dropped. It is stressed that this process inherently produces an almost certainly unrealistically smooth representation of the function being examined. But the resulting curves will at least produce meaningful maximum values of θ_{63}. Superimposed on the diagrams are four θ_{63} values (*A* to *D*) which correspond to different sizes of the *Fd/Fo* ratio (Table 3). The curves in Fig. 9 can now be discussed in terms of the model.

For the curves produced by the $n = 5$ and $n = 10$ filters, the *Fd/Fo* values of 0·3 (level *A*) compares closely with some present-day values, while the two peaks where *Fd/Fo* exceeds unity correspond respectively to departure of the V.G.P. to equatorial latitudes during the polarity transition, and to the later departure or probable non-dipole to dipole relative increase. It is interesting that these peaks can conceivably reflect a true decrease in the dipole field (*Fo*) with the non-dipole field remaining constant. An alternative explanation of increased non-dipole component with a constant dipole field would seem unlikely in view of Coe's (1967) and the Goldstein *et al.* (1968) palaeointensity data.

For the curves produced by the $n = 20$ and 30 filters, the *Fd/Fo* value of 0·3 is not seen, but 0·9 is now the background value, the peak value increasing to about 2·0. The increasing θ_{63} background level could reflect a wobbling dipole superimposed on the secular variation ratio of 0·3 with the peak value showing the effect of diminishing dipole.

Fig. 9 suggests that a secular variation value of *Fd/Fo* of 0·3, which is similar to present-day values, is likely to change to at least 2·0. Using Coe's (1967) mean value of 0·12 G for a palaeointensity (this corresponds to the total field or $Fd+F_{45}$, where F_{45} is the dipole field at 45° North latitude) during the transition the model's dipole and non-dipole fields during the transition can be estimated:

$$\frac{Fd}{Fo} = 1{\cdot}5 \qquad \text{(i)}$$

$$Fd+F_{45} = 0{\cdot}12 \qquad \text{(ii)}$$

$$F_{45} = 1{\cdot}6\, Fo \qquad \text{(iii)}$$

from which $Fo = 0{\cdot}04$ G and $Fd = 0{\cdot}06$ G. If the data of Goldstein *et al.* (1968) is applied, these values are about 0·008 G and 0·012 G, respectively. Thus according

to the model used, the equatorial dipole field may reach as low as two per cent of the present dipole field during the transition for the period represented. The time which this may be is discussed in the following section. To what extent these analyses of the data in terms of Irving & Ward's (1964) model have produced meaningful implications may be resolved by future work.

5. *Limits of the polarity transition*

Estimate of the duration of the period of transition between opposite geomagnetic polarities range from 1000 to 100 000 years. As mentioned above, Cox & Dalrymple (1967) have recently used statistical methods to show that for those reversals which are known to have occurred during the past 4·0 million years the best estimate of the average time for the transition is 4600 years. Since more reversals are likely to be discovered, this figure is very likely to become smaller in similar future calculations. If the limits of transition can be identified in the Steens Mountain section, and if the figure of 4600 years can be applied to this Upper Miocene polarity transition, a precise estimate of the average time interval between successive lavas can be determined. Watkins (1965a) has discussed the various methods used to suggest the duration of between-lava intervals in several areas: these are generally qualitative only, being based on estimates of the time required to accumulate any interbasaltic sediment.

A sound estimate of the average time between lava extrusions, using the duration of a polarity transition must be accompanied by an unambiguous definition of the actual limits of the polarity transition. There are several ways in which the polarity transition limits may be defined, but no one method would alone seem to be satisfactory. The methods which are available are discussed below:

(a) The polarity would experience a complete change if the V.G.P. moved 180° of arc along a palaeolongitude. This would necessitate either a complete lack of, or a hemispherically symmetrical non-dipole component, and this would be unlikely to occur. Such a definition must assume the palaeolongitude direction. Obviously a 180° arc change along an irregular path could conceivably result within the transition itself given a sufficiently active non-dipole activity.

(b) Sigurgeirsson (1957) suggested that the Tertiary geomagnetic field, as recorded in Icelandic lavas, could be considered as transitional if the V.G.P. was equatorward of the present 50° latitude. Application to Fig. 5 would give limits of the transition as lavas 57 and 45. The criterion makes assumptions concerning the position of the ancient axial dipole, which may be problematical for Lower Tertiary and older materials. Nevertheless this would appear to represent the most simple method of defining the limits of a polarity transition. Watkins (1965a) used this method in the preliminary examination of the Steens Mountain data, suggesting that the 60° latitude would be an appropriate limit for Miocene materials. If applied to the data shown in Fig. 5, the transition limits would be lavas 63 and 23.

(c) If the geomagnetic polarity transition is actually the result of a diminishing main dipole intensity, as suggested by several authors, then it should be possible to define the transition limits by determining the ratio of the non-dipole field (*Fd*) to the dipole field (*Fo*). Such a definition, however, requires that the non-dipole field is present throughout the polarity transition period. The relevant palaeointensity data (Coe 1967; Goldstein *et al.* 1968) suggest that the geomagnetic field during the Steens Mountain transition does not diminish to zero intensity, and so it would appear likely that the non-dipole field was present during the transition. The present value of *Fd*/*Fo* varies from 0 in the central Pacific to about 0·4 elsewhere. Inspection of Fig. 9(a) shows that the filters using $n = 5$ and $n = 10$, the results of which are suspected to exhibit the secular variation part of the geomagnetic periodicity spectrum, provide a θ_{63} value of about 8·0 (which is equivalent to an *Fd*/*Fo* value of 0·3)

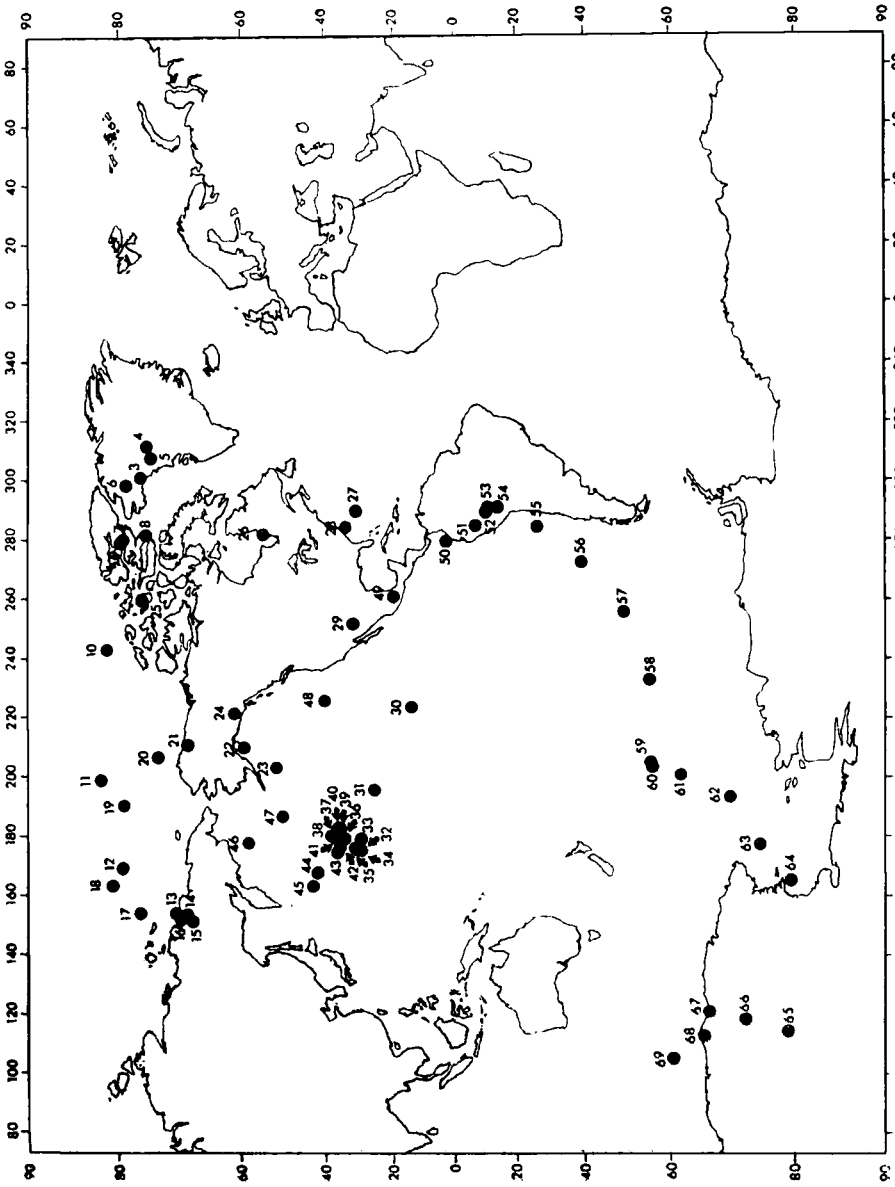

FIG. 10. Mean virtual geomagnetic pole positions for overlapping groups of five successive lavas. The computation procedure is essentially the same as that used to calculate the θ_{63} parameters in Fig. 9. The same limitations as described in the caption of Fig. 9 also apply: an artificial smoothing has been achieved, with independent points occurring for one in every five data points. The number adjacent to each plotted virtual geomagnetic pole position refers to the lava at the centre of the group used to compute the virtual geomagnetic pole position. For additional limitations see text.

in three zones: lavas 1 to 20, 33 to 42, and 66 to the base of the section. The calculation and interpretation of the values of θ_{63} are in the nature of an exploratory exercise and for several reasons are subject to imperfections, but can at least be accepted as providing reasonable minimum estimates of the *Fd/Fo* ratios. Fig. 9 therefore suggests that if a real polarity transition is characterized by *Fd/Fo* values greater than 1·0 (level *B* in Fig. 9), a ' transitional ' situation exists between lavas 45 and 63. Such a definition can only be utilized together with other criteria, however, since θ_{63} values alone obviously cannot distinguish between either different polarities or transitional periods. For example, the similar *Fd/Fo* values greater than 1·0 between lavas 24 and 34 do not involve a change of V.G.P. between high latitudes (Fig. 5) and are therefore not relevant to this particular transition definition.

(d) If the mechanism of the polarity transition is actually a diminishing main dipole, as seems most feasible according to present knowledge, then palaeointensity data would probably provide the most satisfactory means of defining the limits of the polarity transition. No detailed sequential data have yet been published at the time of writing.

It is suggested that each of the four factors discussed above is a necessary but not a sufficient condition for defining the limits of the polarity transition. If the various criteria are considered in inspection of Figs 5 and 9 the limits of the Steens Mountain polarity transition are lavas 28 to 64. These limits include the short duration return of the V.G.P. latitude to equatorial latitudes from almost 50° North, despite the fact that a low θ_{63} value of less than 8·0 (or apparent *Fd/Fo* value of less than 0·3) existed for a finite period during the transition. The alternative choice of the transition limits as lavas 43 to 64 would involve insufficient latitudinal sweep of the V.G.P.

Using the figure of 4600 years (Cox & Dalrymple 1967) as the length of the polarity transition, the suggested limits of lavas 28 to 64 imply an average time interval between lavas of about 130 years. Until the actual duration of the particular polarity transition or details of at least some of the transitions older than 4·0 m.y. are known, it would seem reasonable to accept this figure as correct to within a factor of five. The suggested limits to the average between-lava periods between lavas 28 to 64 on Steen Mountain are therefore from 25 to 650 years. From this, the figure of 0·008 G for the equatorial dipole intensity during the transition would refer to an average value for at least five lavas (four intervals) or from about 100 to 2600 years, although it must be realized that for a given limited period, and with only a non-dipole field present, the value of θ_{63} might still imply a finite value of *Fd/Fo*.

6. *Directional behaviour of the non-dipole field*

Doell & Cox (1965) have used the fact that the non-dipole component is virtually absent in the central Pacific in an attempt to examine the long term behaviour of the dipole field alone. Examination of the non-dipole behaviour can obviously only be made palaeomagnetically where the main dipole field is absent or greatly diminished, as is most likely to be the case during a polarity transition.

If the mechanism of the polarity transition is diminishing stably oriented dipole, then any variation of the position of the V.G.P. away from a palaeolongitude during the transition should represent non-dipole behaviour. This assumption is made for the following analysis.

As in the discussion of the morphology of the polarity transition (Section 4, above) and with the reservations already made, a filtering computational process can provide some evidence of the behaviour of various periodicities of the geomagnetic field. Figs 10–12 show the V.G.P. positions corresponding exactly to three of the four θ_{63} computations in Fig. 9. In the discussion of the significance of the θ_{63} data (Section 4, above) it was argued that filtering with $n = 5$ and 10 was likely to

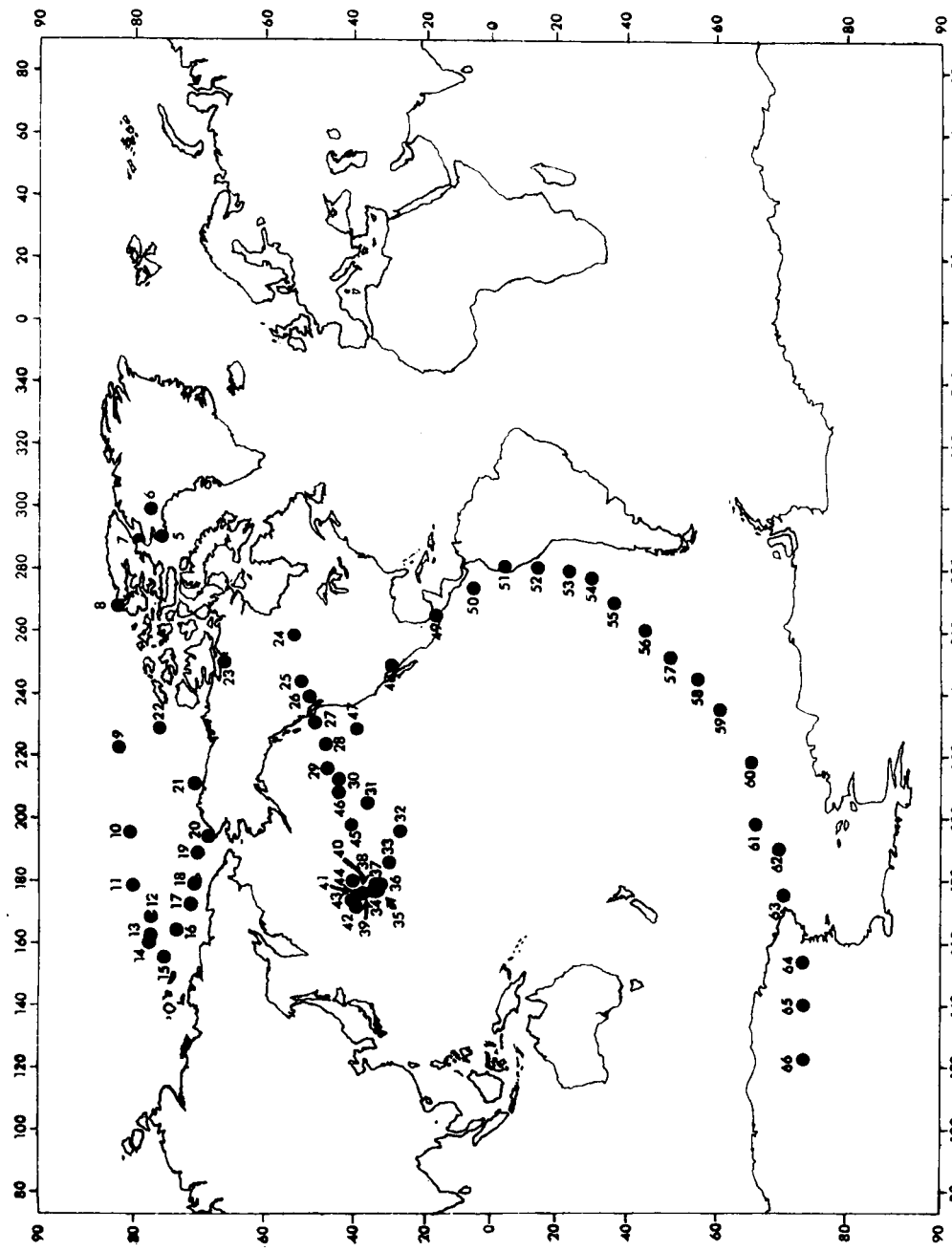

FIG. 11. Mean virtual geomagnetic pole positions for overlapping groups of ten successive lavas. See text and caption of Fig. 9 for explanation of computation procedure and limitations. Independent data points occur only every 10 data points. The number adjacent to each plotted virtual geomagnetic pole position refers to the lava immediately above the centre of each group, which is an interbasaltic horizon.

produce artifical smoothing but nevertheless would preserve evidence of the secular variation behaviour. The estimated average time between successive lavas of 25 to 650 years (Section 5 above) would agree with the suggestion, if the secular variation involves periodicities up to 10 000 years. Therefore Figs 10 and 11 can be interpreted to show a definite eastward swing of the non-dipole components during the polarity transition until equatorial latitudes are reached, when the effect is apparently reversed coincident with the northern migration of the V.G.P. and regrowth of the main dipole influence. If the eastward movement exhibited in Figs 10 and 11 represents an actual non-dipole latitudinal movement of about 120° eastwards during the older half of the transition, and the drifting rate is of the order of present non-dipole movement of 0·20° of latitude per year (Bullard *et al.* 1950) then the transition would occupy about 1200 years, which is less than independent estimates of later periods of transition. If the transition lasted the order of 4600 years the data could also be explained by a non-dipole latitudinal drift of about 0·05° latitude per year during the transition.

Fig. 11 also shows that following the polarity transition, the filtered V.G.P. positions make an anticlockwise rotation around a position north of the Bering Sea. This motion, with a much smaller radius of curvature than the suggested dominantly non-dipole behaviour during the transition proper at much lower latitudes, could represent the lower relative contribution of the non-dipole field to the total field which would be dominantly dipolar following the transition, as argued in Section 4 (above). With filters of wider values than $n = 5$ and 10, it might be expected that the effect of the non-dipole field will become suppressed. Fig. 12 shows that with $n = 20$, the apparent eastward non-dipole drift feature is considerably diminished. The artificially smoothed path of the successive V.G.P. positions in Fig. 12 *could* reflect the V.G.P. due dominantly to a diminishing and reversing dipole although it must be stressed that only three totally independent points exist in Fig. 12.

A geomagnetic pole, or surface expression of the geocentric dipole, for the period involved is inferred to be in the region 210° east, 80° north (Fig. 12). Because of the fact that the corresponding reversed geomagnetic pole, which existed prior to the initiation of the polarity change was not at 30° East, 80° South, it can be stated that the observed polarity change does not possess perfect symmetry. An almost identical result has been presented by Ito & Fuller (1968), who show that a Lower Pliocene reversed to normal polarity transition recorded in a plutonic body in Oregon also shows a V.G.P. path confined to the Pacfic, with the V.G.P. positions during the later stages being clustered in the area just north of the Bering Sea.

As mentioned earlier Ito & Fuller's (1968) transition also records the ' rebound effect ' in which the palaeomagnetic inclination approached zero for a limited period shortly after the V.G.P. has moved from southern to northern latitudes. This double similarity provides a most intriguing and obvious suggestion: according to the two independent studies, there exists the possibility that the mechanism involving changes of polarity from reversed to normal state was not greatly different in terms of V.G.P. behaviour at 8·2 m.y. (Ito & Fuller, 1968) ago and 15·1 m.y. ago (Baksi *et al.* 1967) in Oregon. An additional detailed study of another polarity reversal in Oregon may assist in determining whether or not the double similarity described is meaningful or sheer coincidence, which must at this stage be considered as the most likely explanation.

The suggested average time between lavas (Section 5, above) can be used to infer the period of the geomagnetic field movements discussed. It is suggested then, that the departure of the V.G.P. to equatorial regions or the ' rebound effect ' during the final phases of the transition might reflect a geomagnetic field behaviour as short as 125 or as much as 3300 years in total (five interbasaltic horizons, as shown in Fig. 4). Geological intuition, based on observation of the nature of the surfaces of the lavas

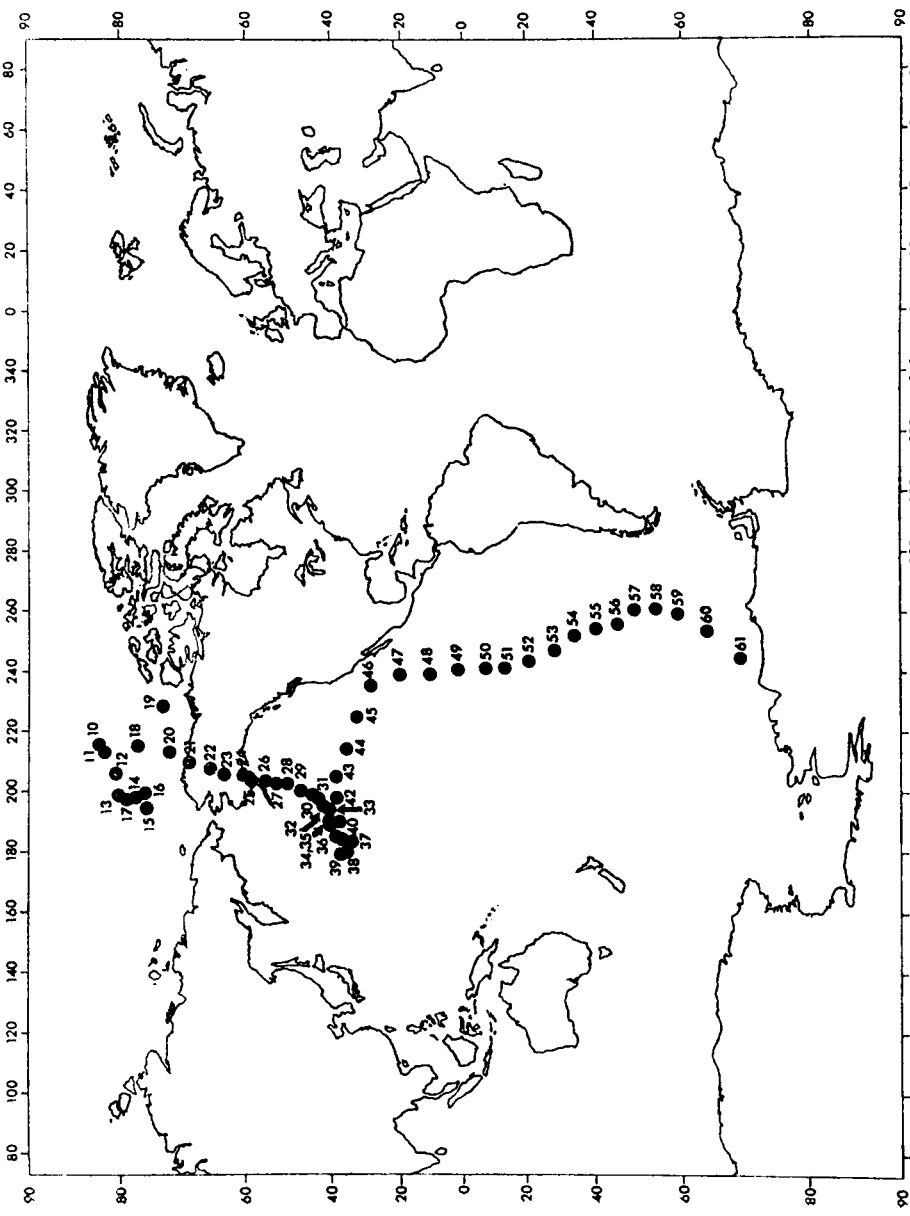

FIG. 12. Mean virtual geomagnetic pole positions for overlapping groups of twenty successive lavas. See text and caption of Fig. 9 for explanation of computation procedure and limitations. Independent data points occur only every 20 data points. The number adjacent to each plotted virtual geomagnetic pole position refers to the lava immediately above the centre of each group, which is an interbasaltic horizon.

sampled, would tend to favour the former estimate as a limit closer to the real time involved. This is much shorter than the observed periods of intensity fluctuations of the Earth's dipole field, which are of the order of 10 000 years (Cox 1968, p. 3248), but is similar to the period of oscillation of Rikitake's (1958) twin disc dynamo, which is of the order of 50 years when computed in terms of the properties of the Earth (Allan 1962). This observation could be explained, then, by a simple twin disc dynamo simulating the geomagnetic field only when the main dipole field is diminished.

Conclusions

The directions of remanent magnetism in a sequence of Upper Miocene lavas collected from Steens Mountain are due to ambient magnetic field during the initial cooling. The normal polarity lavas, which make up most of the section, do not show any preferred association with low or high oxidation state titanomagnetites.

No major time breaks exist on the section, which has recorded a change from reversed to normal geomagnetic polarity. The path of the virtual geomagnetic pole, when averaged, is confined to the Pacific region. A period of apparent dipolar instability or growth in non-dipole component during the final phases of the polarity change caused a rapid departure of the virtual geomagnetic pole to southern equatorial latitudes prior to restoration of the northerly drift of the virtual geomagnetic pole. Because a similar observation has been made in the case of another, but younger, palaeomagnetic reversal in Oregon (Ito & Fuller 1968), it is suggested that this 'rebound effect' may be a fundamental aspect of the geomagnetic reversal process. More data can resolve this possibility.

The latitude variation of the virtual geomagnetic pole, and the relation of the circular standard deviation (θ_{63}) to a geomagnetic field model have been considered in defining the limits of the polarity transition which is interpreted to span 36 lavas. Comparison with independent ideas about the duration of polarity transitions during the past 4·0 million years provides an estimate of the average time between successive lavas of approximately 130 years, which indicates a duration of less than 1000 years for the large departure of the virtual geomagnetic pole from high latitudes equatorwards and back to high latitudes during final phases of the transition. Both V.G.P. longitudinal depature (Fig. 11) and a more rapidly moving geomagnetic field (Fig. 7) existed during the transition. When added to the palaeointensity results, these facts show that the departure and the major migration of the virtual geomagnetic pole from southern to northern latitudes are best interpreted to be due to increased dominance of the more rapidly moving non-dipole field, as a result of a decreased main dipole component. An exploratory application of Irving & Ward's (1964) geomagnetic field model to the data produces results consistent with a ratio of non-dipole (*Fd*) to equatorial dipole field (*Fo*) of 0·3 (which is similar to present values) occurring before and after the polarity transition, and also shortly before the final phase of dipolar instability within the polarity transition. Together with independently obtained palaeointensity results, an average equatorial dipole intensity as low as 0·008 G for not less than 100 years during the transition is suggested by the model.

Application of a filtering computation to the data indicates that an eastward drifting non-dipole component was present during the transition. As the polarity transition was completed, the easterly drift of the non-dipole component was masked by the growth of geomagnetic field components with longer periodicities, one of which apparently caused a clockwise rotation of the V.G.P. (when viewed on a north polar projection) around a point north of the Bering Strait. The easterly drifting non-dipolar component may have moved at only 0·05° of latitude per year: but if it drifted at rates similar to the present then the duration of the polarity transition was about 1200 years. If this is so, then the average time between successive lava flows would be only about 30 years; the duration of large departure of the virtual geo-

magnetic pole during the final phases of the polarity transition would be only about 150 years; and the period when the average dipole intensity was as low as 0·008 G (or about two per cent of the present field) would be 120 years. Because of the fact that the transition took place during the Upper Miocene, exact determination of the average time between successive lavas which would assist in resolving some of these ambiguities is not realistic. The suggested limits would appear reasonable however, in view of the complete absence of interbasaltic soils in the section. The 71 successive lavas of the Steens Mountain section therefore probably accumulated in a period of about 2000 to 50 000 years.

Acknowledgments

The field work was supported by N.S.F. grant number GF-76, as part of the U.S.–Japan co-operation programme. The laboratory work was also supported in part by this grant. Acknowledgments are due to the U.S. Geological Survey for access to apparatus used during the initial phases of the laboratory study. Most of the laboratory work was carried out using apparatus provided in part by the National Science Foundation grants number Ga 582 and Ga 602. The computing centre at Florida State University is gratefully acknowledged for the provision of much computer time on their CDC 6400. Dr. D. W. Strangway kindly provided a preprint of one of his papers.

Department of Geology,
Florida State University,
Tallahassee,
Florida 32306.

1968 *November.*

References

Ade-Hall, J., Wilson, R. L. & Smith, P. J., 1965. The petrology, Curie points, and natural magnetizations of basic lavas, *Geophys. J. R. astr. Soc.*, 323–336.

Aitken, M. J., Harold, M. R. & Weaver, G. H., 1964. Some archaeomagnetic evidence concerning the secular variation in Britain, *Nature, Lond.*, **201,** 659–660.

Allan, D. W., 1958. Reversals of the Earth's magnetic field, *Nature, Lond.*, **182,** 469–470.

Baksi, A. K., York, D. & Watkins, N. D., 1967. Age of the Steens Mountain geomagnetic polarity transition, *J. geophys. Res.*, **72,** 6299–6308.

Blackett, P. M. S., 1962. On distinguishing self-reversal from field-reversed rocks, *J. Phys.. Soc. Jap.*, **17,** 699–705.

Buddington, A. F. & Lindsley, D. H., 1964. Iron–titanium oxides and synthetic equivalents, *J. Petrol.*, **5,** 310–357.

Bullard, E. C., 1968. Reversals of the Earth's magnetic field, *Phil. Trans. R. Soc.*, **A263,** 481–524.

Bullard, E. C., Freedman, C., Gellman, H. & Nixon, J., 1950. The westward drift of the Earth's magnetic field, *Phil. Trans. R. Soc.*, **A243,** 67–92.

Coe, R. S., 1967. Paleo-intensities of the Earth's magnetic field determined from tertiary and quaternary rocks, *J. geophys. Res.*, **72,** 3247–3262.

Cox, A. V., 1962. Analysis of present geomagnetic field for comparison with paleomagnetic results, *J. Geomagn. Geoelect.*, **13,** 101–112.

Cox, A. V., 1966. Geomagnetic secular variation in Alaska, *Trans. Am. geophys. Un.*, **47,** 78.

Cox, A. V., 1968. Lengths of geomagnetic polarity intervals, *J. geophys. Res.*, **73,** 3427–3460.

Cox, A. & Dalrymple, G. B., 1967. Statistical analysis of geomagnetic reversal data and the precision of potassium–argon dating, *J. geophys. Res.*, **72,** 2603–2614.

Cox, A. & Doell, R. R., 1964. Long period variation in the geomagnetic field, *Bull. seism. Soc. Am.*, **54,** 2243–2270.

Currie, R. G., Gromme, E. S. & Verhoogen, J., 1963. Remanent magnetization of some Upper Cretaceous granitic plutons in the Sierra Nevada, California, *J. geophys. Res.*, **68,** 2263–2280.

Dagley, P., Wilson, R. L., Walker, G. P. L., Watkins, N. D., Sigurgiersson, T., Haggerty, S. E., Smith, P. J., Edwards, J., Ade-Hall, J. & Grasty, R. L., 1967. Geomagnetic polarity zones for Icelandic lavas, *Nature, Lond.*, **216,** 25–29.

Doell, R. R., 1968. Paleomagnetic studies of lavas of the islands of Kauai and Oahu, *Trans. Am. geophys. Un.*, **49,** 127.

Doell, R. R. & Cox, A., 1961. Paleomagnetism, *Adv. Geophys.*, **8,** 221–313.

Doell, R. R. & Cox, A., 1963. The accuracy of the paleomagnetic method as evaluated from historic Hawaiian lava flows, *J. geophys. Res.*, **68,** 1997–2009.

Doell, R. R. & Cox, A., 1965. Paleomagnetism of Hawaiian lava flows, *J. geophys. Res.*, **70,** 3377–3405.

Doell, R. R. & Cox, A., 1967. Analysis of alternating field demagnetization equipment, in *Methods in Paleomagnetism*, pp. 241–253, ed. by D. W. Collinson, K. M. Creer and S. K. Runcorn, Elsevier, Amsterdam.

DuBois, R. L., 1967. Archaeomagnetism and secular variation in the past 2000 years, *Trans. Am. geophys. Un.*, **48,** 79.

Evernden, J. F. & James, G. T., 1964. Potassium–argon dates and tertiary floras of North America, *Am. J. Sci.*, **262,** 945–974.

Fisher, R., 1953. Disperson on a sphere, *Proc. R. Soc.*, **A217,** 295–305.

Fuller, R. R., 1931. The geomorphology and volcanic sequence of Steens Mountain in southeastern Oregon, *Univ. Wash. Publs Geol.*, **3,** 1–130.

Goldstein, M. A., Larson, E. E. & Strangway, D. W., 1968. A paleomagnetic study of a Miocene transition zone in southeastern Oregon, *Trans. Am. geophys. Un.*, **49,** 127–128; Paleomagnetism of a Miocene transition zone in Southeastern Oregon, *J. geophys. Res.*, submitted for publication.

Grommé, C. S., 1965. Anomalous and reversed paleomagnetic field directions from the Miocene Lovejoy Basalt, northern California, *J. Geomagn. Geoelect.*, **17,** 445–457.

Haggerty, S. E. & Baker, I., 1967. The alteration of olivine in basaltic and associated lavas—I. High temperature alteration, *Contr. Miner. Petrol*, **16,** 233–257.

Heinrichs, D. F., 1967. Paleomagnetism of the Plio-Pleistocene Lousetown formation, Virginia City, Nevada, *J. geophys. Res.*, **72,** 3277–3294.

Irving, E., 1964. *Paleomagnetism and Its Application to Geological and Geophysical Problems*, 399 pp., John Wiley, New York.

Irving, E. & Ward, M. A., 1964. A statistical model of the geomagnetic field, *Geofis. pura Appl.*, **57,** 25–30.

Ito, H. & Fuller, M., 1968. A paleomagnetic study of a reversal of the Earth's magnetic field, *Trans. Am. geophys. Un.*, **49,** 127.

Kahle, A. B., Ball, R. H. & Vestine, E. H., 1967. Comparison of estimates of surface fluid motions of the Earth's core for various epochs, *J. geophys. Res.*, **72,** 4917–4925.

Kawai, N., Hirooka, K. & Tokieda, K., 1967. A vibration of geomagnetic axis around the geographic north pole in historic time, *Earth planet. Sci. Lett.*, **3,** 48–50.

Larson, E. E. & Strangway, D. W., 1968. Discussion of a paper entitled ' Correlation of petrology and natural magnetic polarity in Columbia River basalts ' by R. L. Wilson and N. D. Watkins, *Geophys. J. R. astr. Soc.*, **15,** 437.

Lindsley, D. H., 1965. Lower thermal stability of $FeTi_2O_5$–Fe_2TiO_5 (Pseudobrookite) solid solution series, Geol. Soc. Am., Program, Annual Meeting, 96 (abstract).

Mathews, J. H. & Gardner, W. K., 1963. Field reversals of 'paleomagnetic' type in coupled disk dynamos, *U.S. Naval Res. Lab. Rept.*, No. 5886, 1.

McDonald, K. L. & Gunst, R. H., 1968. Recent trends in the Earth's magnetic field, *J. geophys. Res.*, **73**, 2057–2069.

McElhinny, M. W., 1966. An improved method for demagnetizing rocks in alternating magnetic fields, *Geophys. J. R. astr. Soc.*, **10**, 369–374.

McMahon, B. E. & Strangway, D. W., 1967. Kiaman magnetic interval in the western United States, *Science*, **155**, 1012–1013.

Ninkovich, D., Opdyke, N., Heezen, B. C. & Foster, J. H., 1966. Paleomagnetic stratigraphy rates of deposition, and tephrachronology in North Pacific deep-sea sediments, *Earth Planet. Sci. Lett.*, **1**, 476.

Patton, B. J. & Fitch, J. L., 1962. Anysteretic remanent magnetization in small steady fields, *J. geophys. Res.*, **67**, 307–311.

Prévot, M. & Watkins, N. D., 1969. Essais de détermination de l'intensité du champ magnétique terrestre au cours d'un reversement de polarité, *Ann. Geophys.*, in press.

Rikitake, T., 1958. Oscillations of a system of disk dynamos, *Proc. Camb. phil. Soc. math. phys. Sci.*, **54**, 89–105.

Rikitake, T., 1966. *Electromagnetism and the Earth's Interior*, 308 pp., Elsevier, Amsterdam.

Runcorn, S. K., 1959. On the theory of geomagnetic secular variation, *Ann. Geophys.*, **15**, 87–92.

Sigurgeirsson, Th., 1957. Direction of magnetization in Icelandic basalts, *Phil. Mag., Suppl. adv. Phys.*, **6**, 240–246.

Smith, P. J., 1967. The intensity of the ancient geomagnetic field: a review and analysis, *Geophys J. R. astr. Soc.*, **12**, 321–362.

Smith, P. J., 1968. Paleomagnetism and the compositions of highly-oxidized iron–titanium oxides in basalts, *Phys. Earth. planet. Inter.*, **1**, 88–92.

Smith, P. J. & Needham, J., 1967. Magnetic declination in medieval China, *Nature, Lond.*, **214**, 1213–1214.

Strangway, D. W. & Larson, E. E., 1965. A paleomagnetic study of some late Cenozoic basalts from Oregon, *Trans. Am. geophys. Un.*, **46**, 66–67.

Uyeda, S., Fuller, M. D., Belshé, J. T. C. & Girdler, R. W., 1963. Anistropy of magnetic susceptibility of rocks and minerals, *J. geophys. Res.*, **68**, 279–291.

Walker, G. W. & Repenning, C. A., 1965. Reconnaissance geologic map of the Adel quadrangle, Lake, Harney, and Malheur counties, Oregon, *U.S. Geol. Surv. Misc. Geol. Invest.*, Map 1–446.

Watkins, N. D., 1963. The behaviour of the geomagnetic field during the Miocene period in southeastern Oregon, *Nature, Lond.*, **197**, 126–128.

Watkins, N. D., 1965a. Frequency of extrusions of some Miocene lavas in Oregon during an apparent transition of the polarity of the geomagnetic field, *Nature, Lond.*, **206**, 801–803.

Watkins, N. D., 1965b. Paleomagnetism of the Columbia Plateaus, *J. geophys. Res.*, **70**, 1379–1406.

Watkins, N. D., 1965c. A palaeomagnetic observation of Miocene geomagnetic secular variation in Oregon, *Nature, Lond.*, **206**, 879–882.

Watkins, N. D., 1967. Unstable components and paleomagnetic evidence for a geomagnetic polarity transition, *J. Geomagn. Geoelect.*, **19**, 63–76.

Watkins, N.D., 1968a. Short-period geomagnetic polarity events in deep-sea sedimentary cores, *Earth planet. Sci. Lett.*, **4**, 341–346.

Watkins, N. D., 1968b. Reply to comments by E. E. Larson and D. W. Strangway on a paper by R. L. Wilson and N. D. Watkins entitled ' Correlation of petrology and natural magnetic polarity in Columbia Plateau basalts ', *Geophys. J. R. astr. Soc.*, **15,** 444.

Watkins, N. D. & Haggerty, S. E., 1967. Primary oxidation variation and petrogenesis in a single lava, *Contr. mineral. Petrol.*, **15,** 251–271.

Watkins, N. D. & Haggerty, S. E., 1968. Oxidation and magnetic polarity in single Icelamdic lavas and dikes, *Geophys. J. R. astr. Soc.*, **15,** 305–316.

Wensink, H., 1964. Secular variation of Earth magnetism in Plio-Pleistocene basalts of eastern Iceland, *Geol. Mijnbouw*, **43,** 403–413.

Wilson, R. L., 1968. Reply to comments by E. E. Larson and D. W. Strangway on a paper by R. L. Wilson and N. D. Watkins entitled ' Correlation of petrology and natural magnetic polarity in Columbia Plateau basalts ', *Geophys. J. R. astr. Soc.*, **15,** 443.

Wilson, R. L. & Watkins, N. D., 1967. Correlation of petrology and natural magnetic polarity in Columbia Plateau basalts, *Geophys. J. R. astr. Soc.*, **12,** 405–424.

Wilson, R. L., Haggerty, S. E., & Watkins, N. D., 1968. Variation of palaeomagnetic stability and other parameters in a vertical traverse of a single Icelandic lava, *Geophys. J. R. astr. Soc.*, **16,** 287–304.